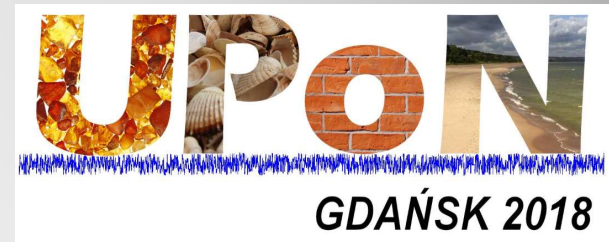


Macroscopic random telegraph noise



Grzegorz Jung

Physics Department, Ben Gurion University of the Negev

and

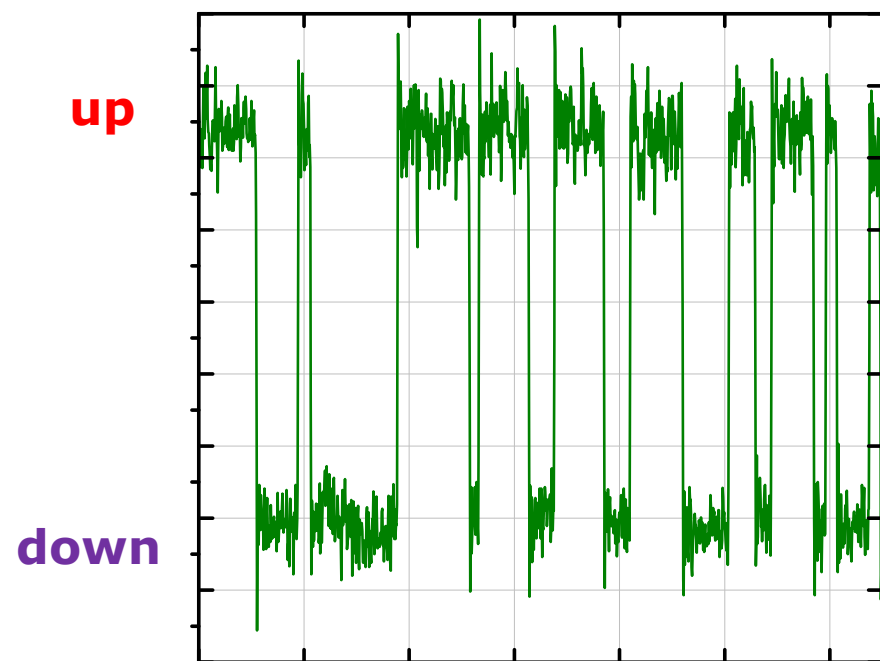
Institute of Physics, Polish Academy of Sciences



Outline

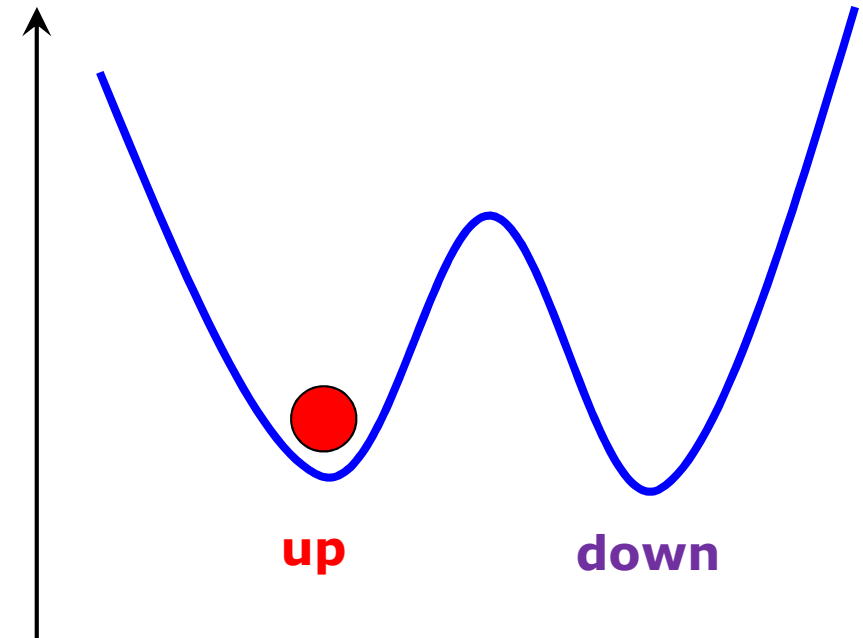
- **Macroscopic Random Telegraph Noise (M-RTN)**
- **M-RTN in superconductors**
 - **Vortex dissipation, vortex phase transitions**
 - **Edge contamination**
 - **Superconducting M-RTN UPON features explained?**
- **M-RTN in magneto-resistive manganites**
 - **Robust M-RTN**
 - **Dynamic current redistribution and M-RTN**
 - **Meyer-Neldel rule behind robust M-RTN in manganites**

Random Telegraph Noise



RTN time trace

Energy



**Two-Level Fluctuator
TLF**

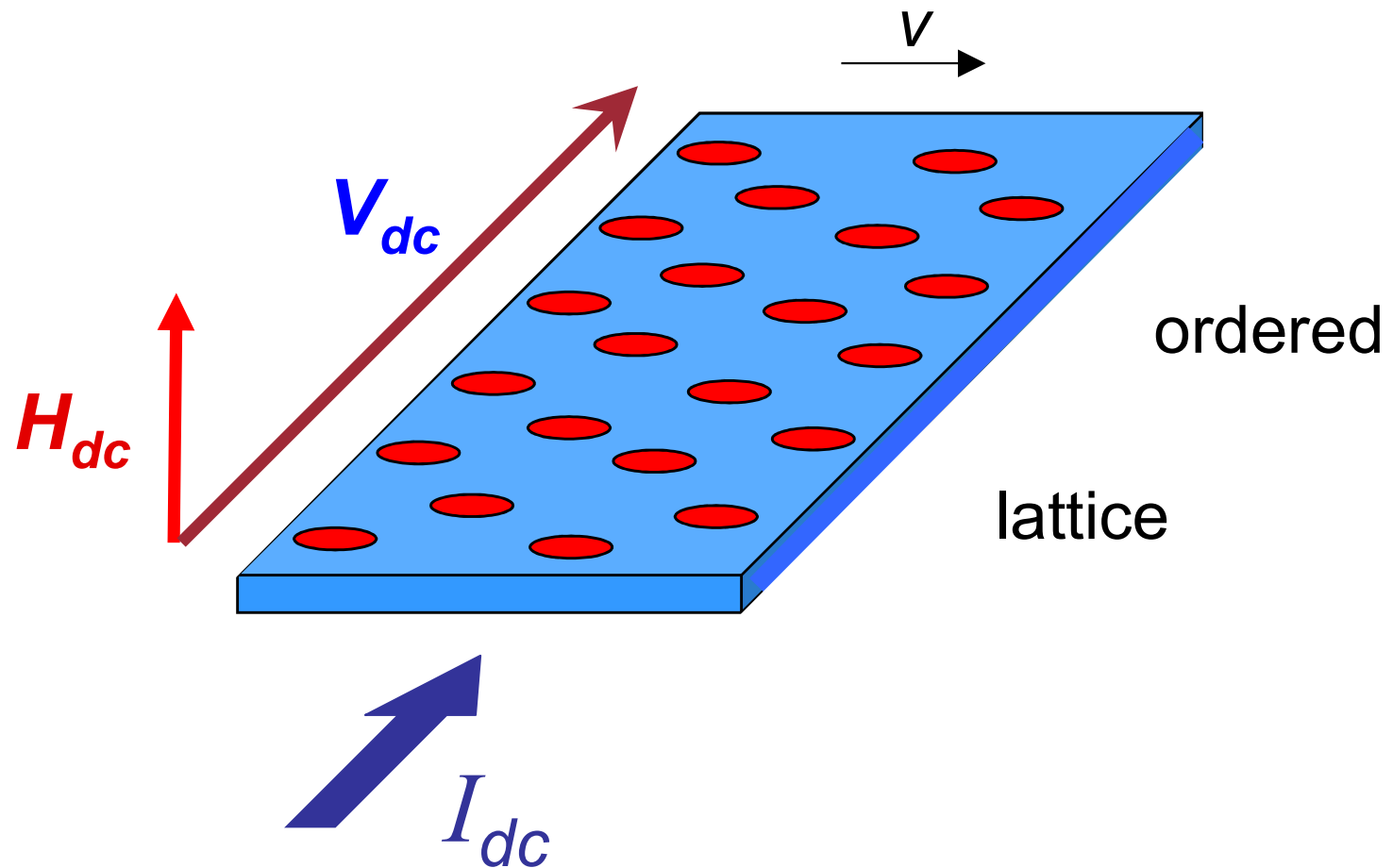
Macroscopic Random Telegraph Noise

- RTN typically appears in conductivity of mesoscopic systems due to action of elementary TLF, such as defects capable of trapping/detrapping charge carriers. Incoherent superposition of elementary TLFs with a flat distribution of activation energies leads to 1/f noise.
- In strongly correlated electronic systems, such as HTSC cuprates or CMR manganites, RTN shows out also in macroscopically large samples.
- Macroscopic RTN cannot be due to an elementary TLF, associated with a single defect, but to a macroscopic size TLF capable of changing the state of the system on the length scale comparable with the size of the investigated system.

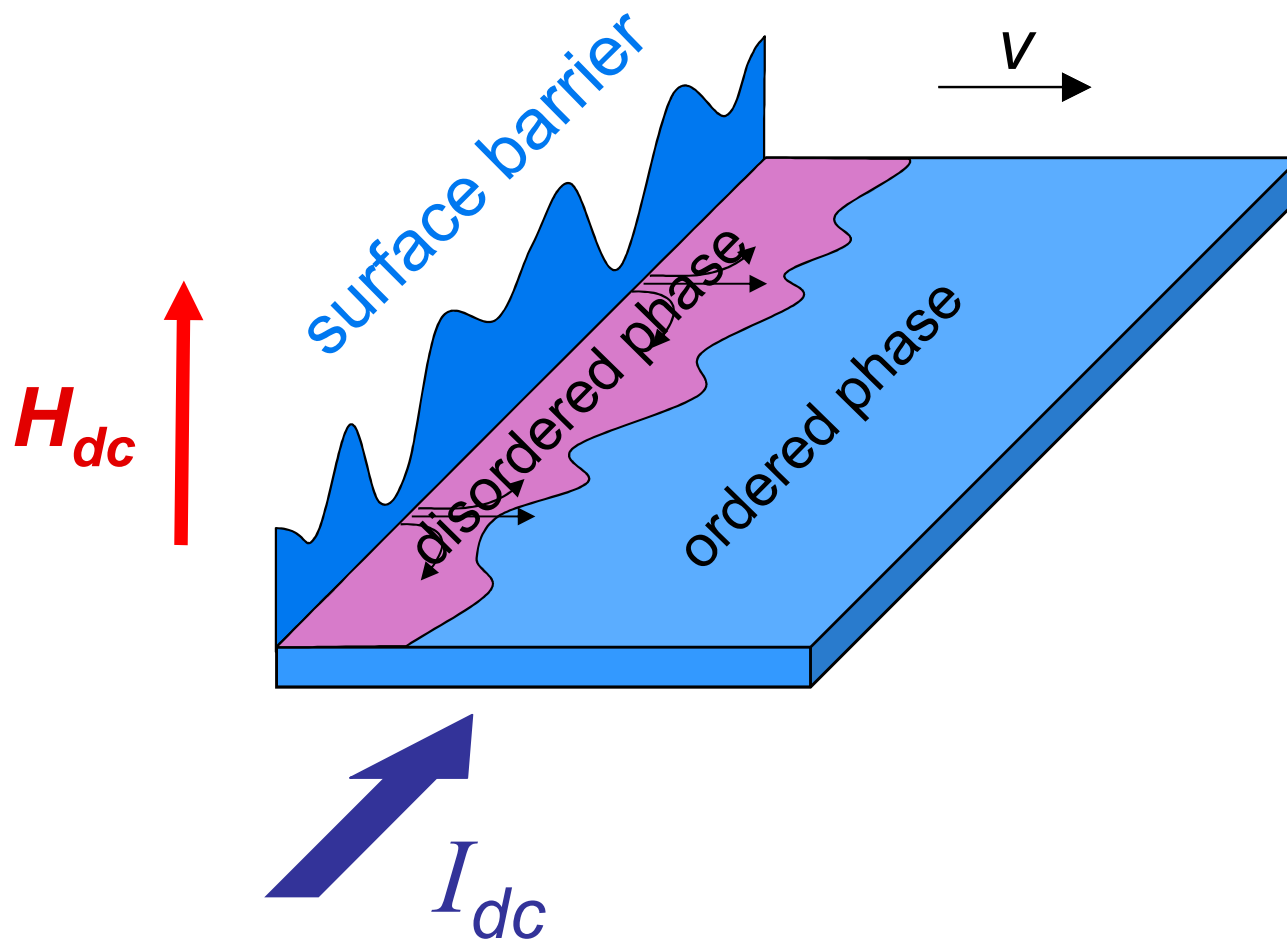
Macroscopic RTN in superconductors

- Macroscopic RTN appears in low-T_c and high-T_c superconductors, in granular, and in homogenous single crystalline bulk and thin film samples.
- Macroscopic telegraph noise is more pronounced in HTSC mostly because of higher temperatures of operation.
- The prime suspect: moving vortex matter and vortex phase transition

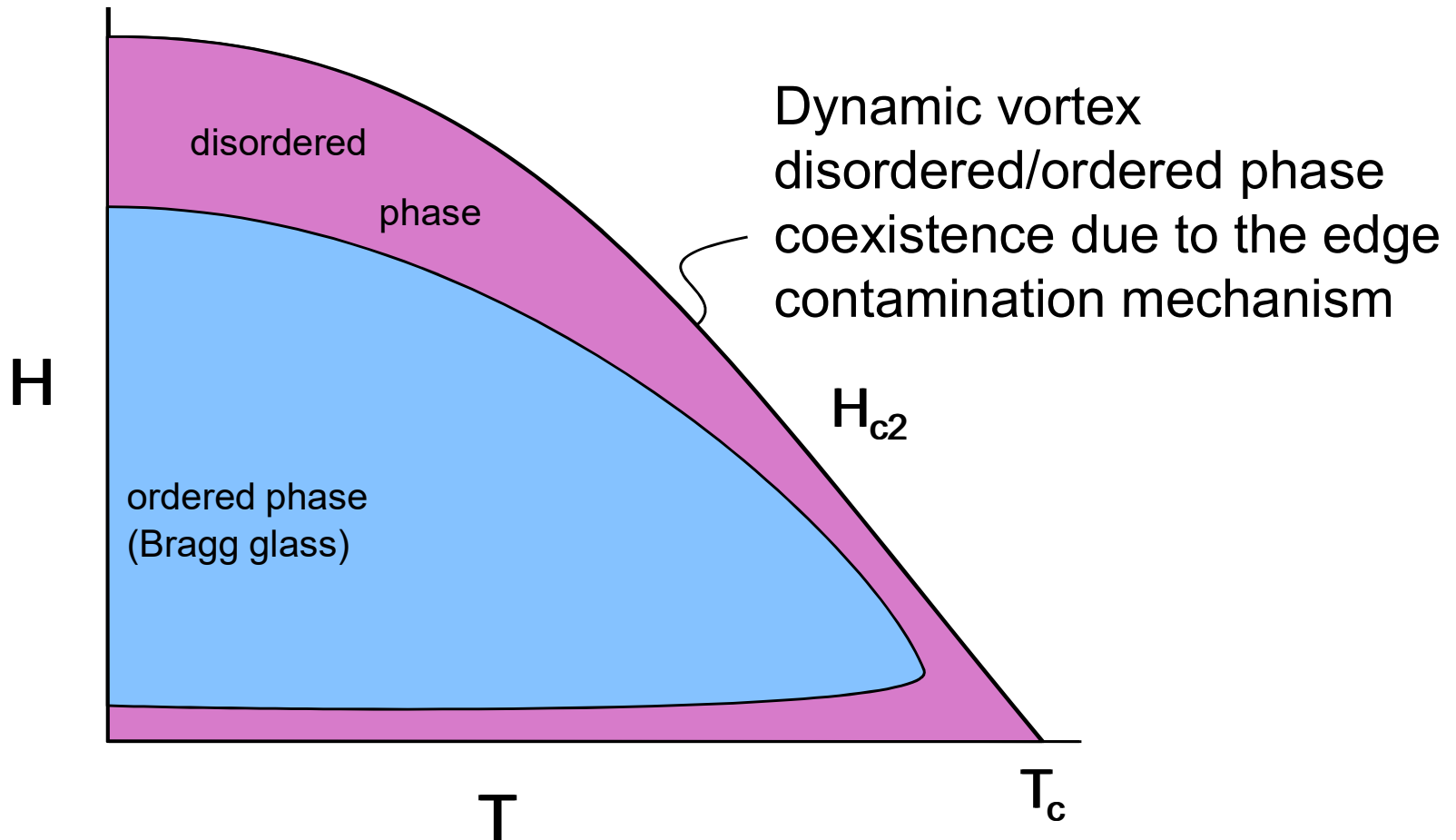
Dissipation in a superconducting state



Edge contamination mechanism

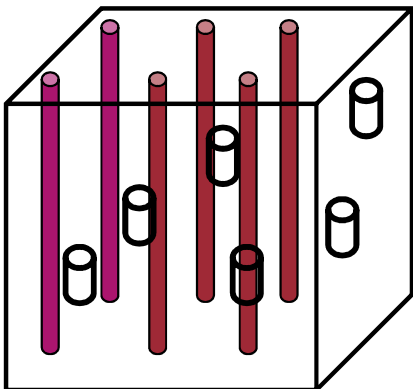


Vortex phase diagram



Vortex matter phases

Ordered Phase



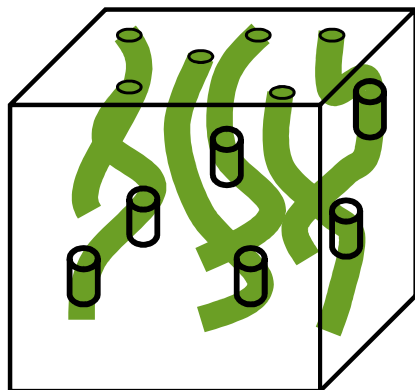
Elastic energy
dominating

$$R_f = n R_N \Phi_0 / \mu_0 H_{c2}$$

Weakly pinned,
lower critical current

Lower vortex density,
lower R_f

Disordered Phase

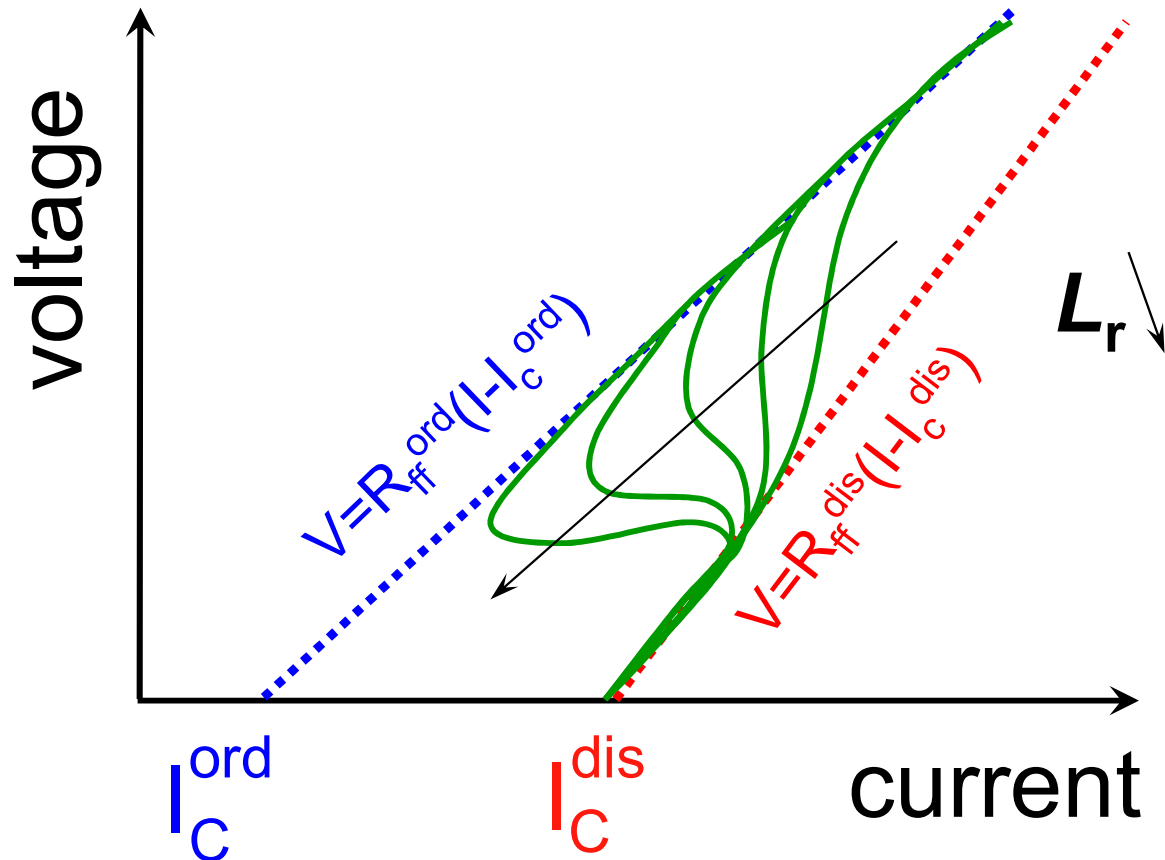


Pinning energy
dominating

Strongly pinned,
higher critical current

Higher vortex density,
higher R_f

I-V curves of coexisting phases



$$R_f^{\text{dis}} > R_f^{\text{ord}}$$

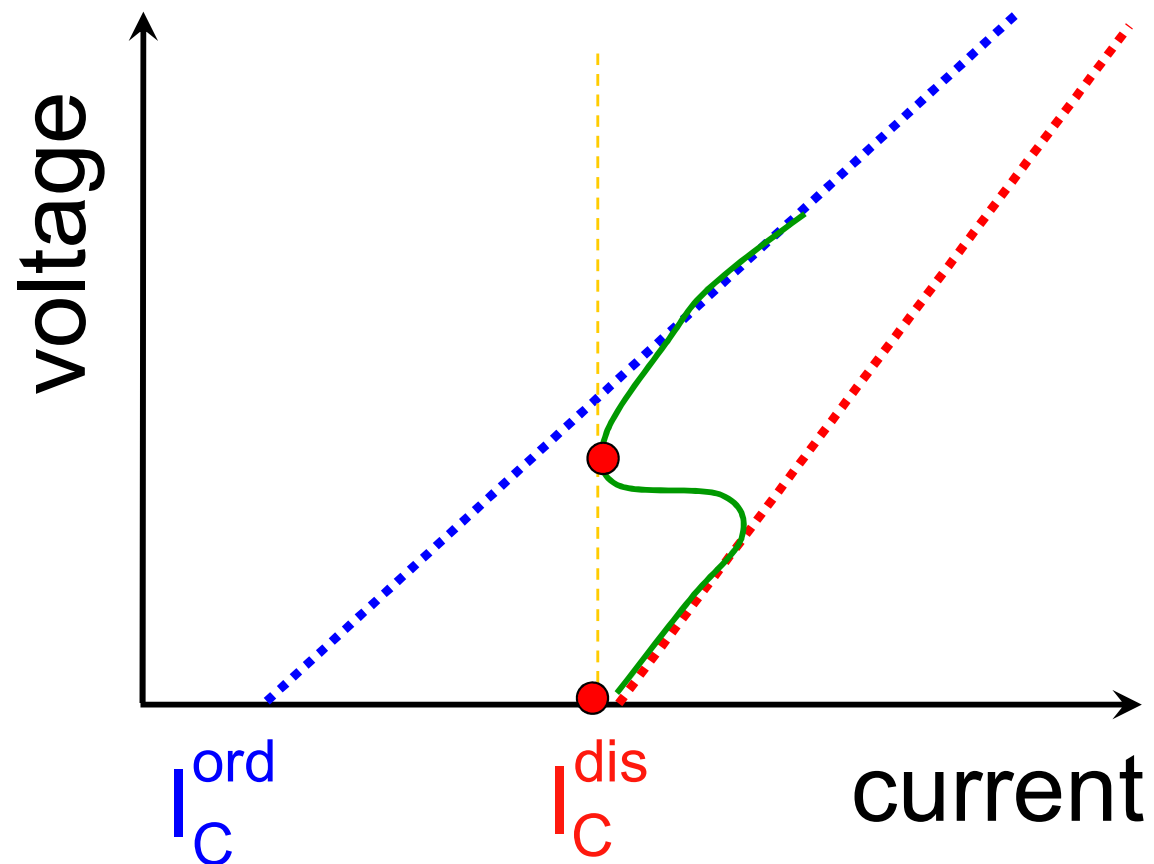
$$I_C^{\text{dis}} > I_C^{\text{ord}}$$

$$L_r \approx L_0 \left(\frac{v_0}{v} \right)^\alpha$$

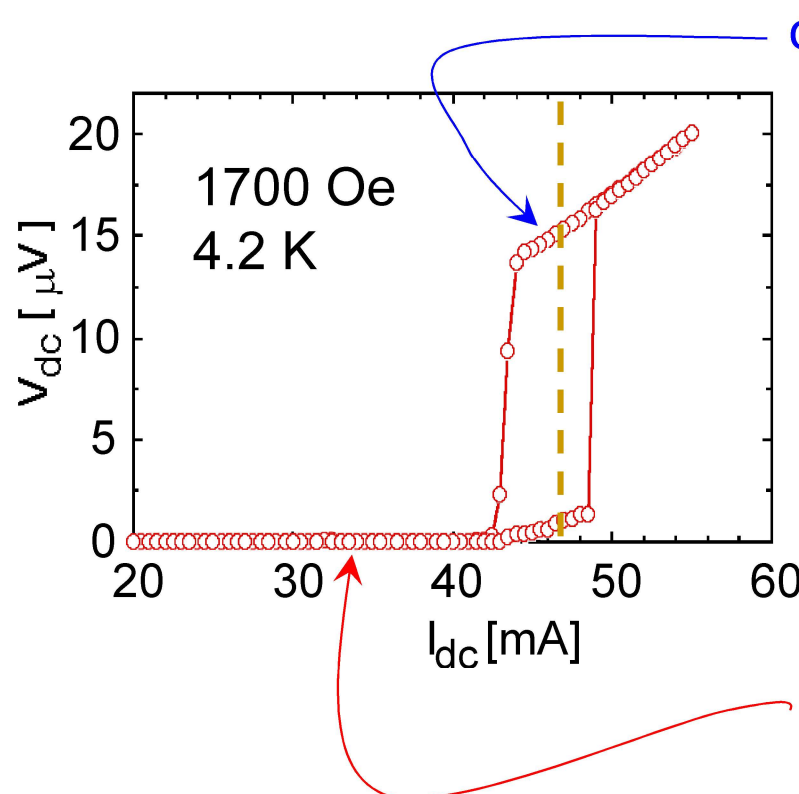
$$L_r \approx L_0 \left(\frac{V_0}{V} \right)^\alpha$$

$$\alpha \approx 1-3$$

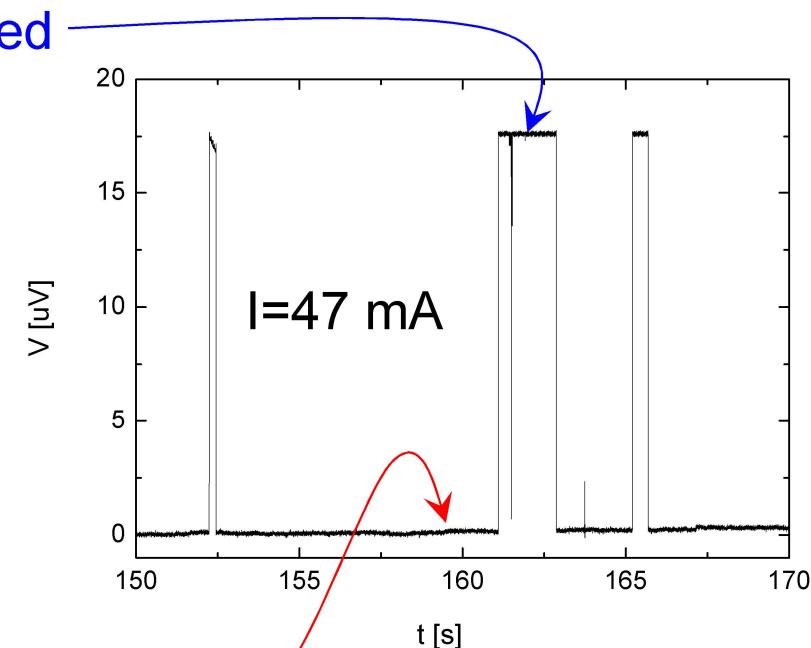
S-shaped I - V curves and M-RTN



M-RTN in NbSe₂ single crystal

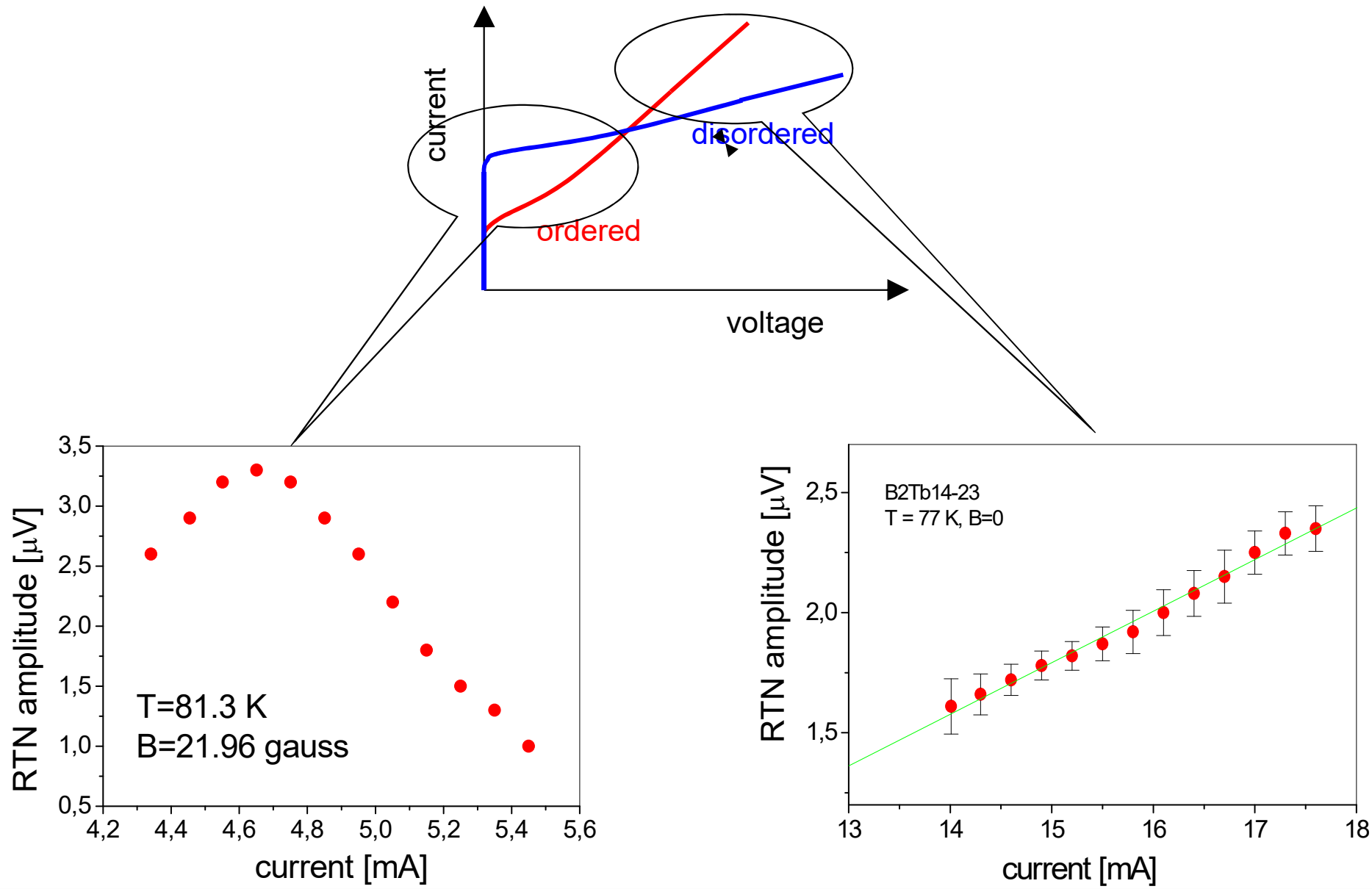


S-shaped I-V curve

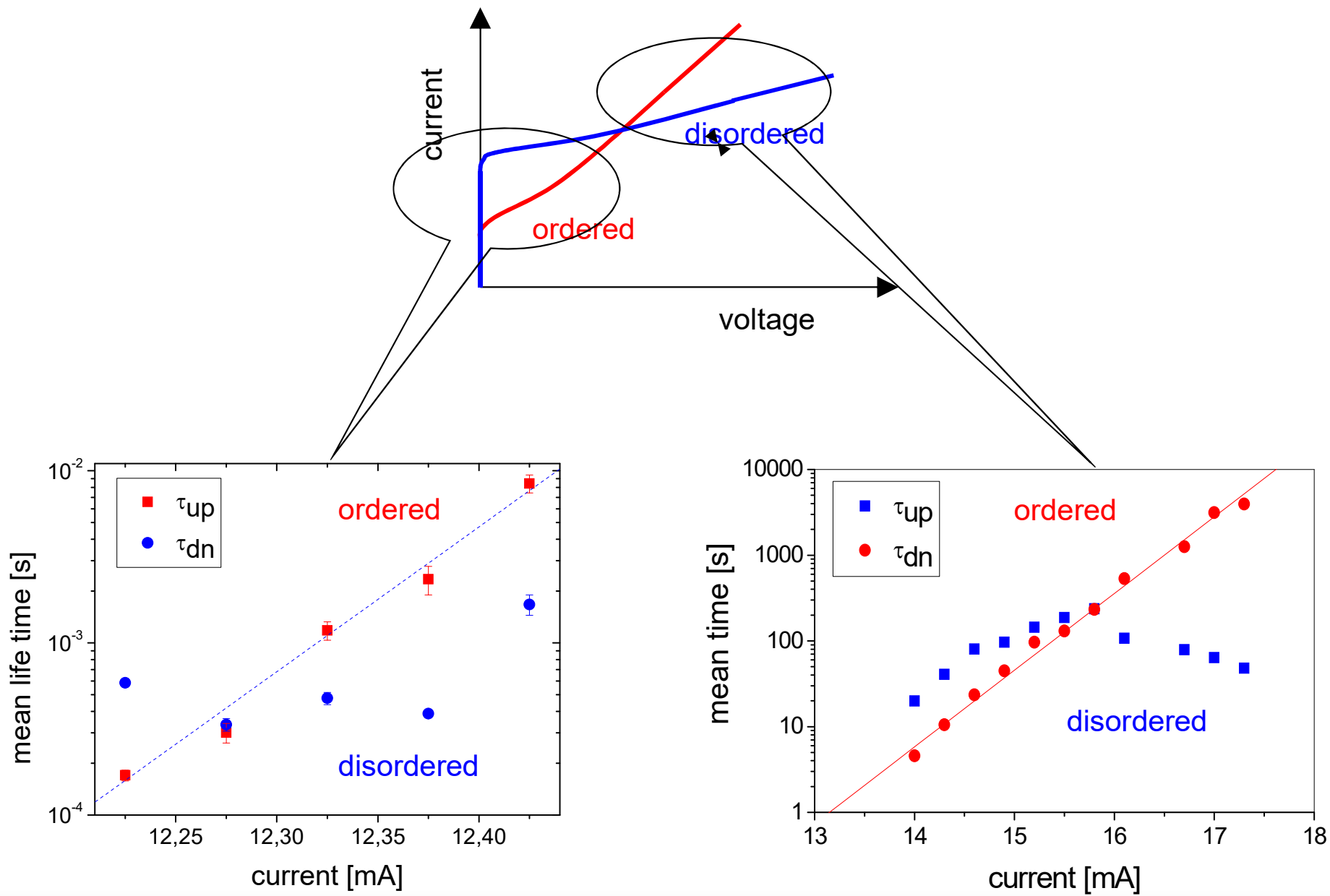


time domain voltage

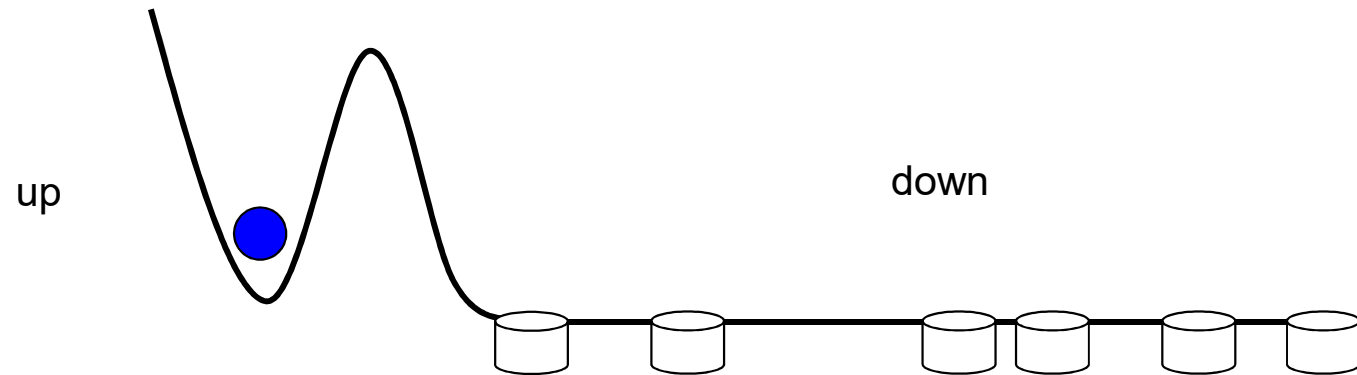
M-RTN amplitudes BSCCO



M-RTN average lifetimes BSCCO

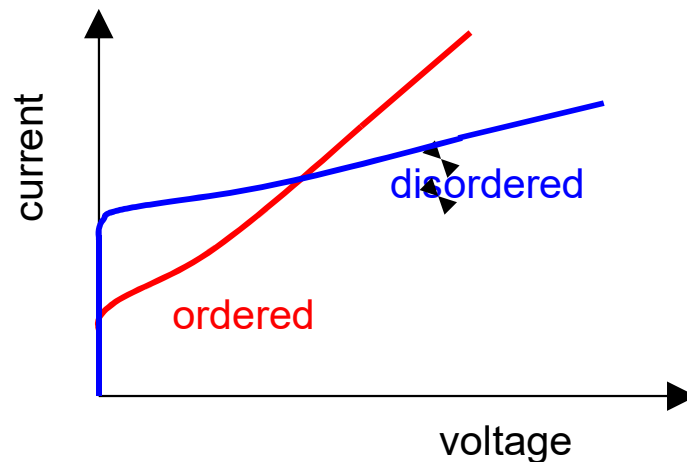


Single well M-RTN fluctuator

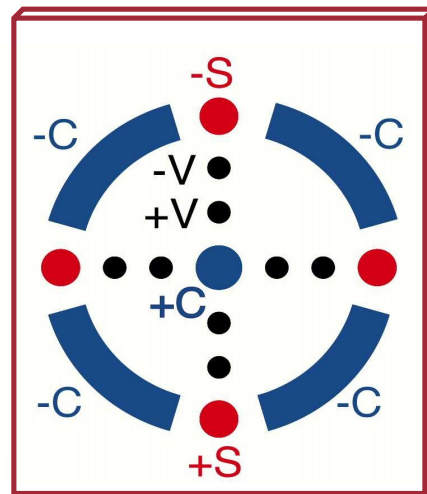
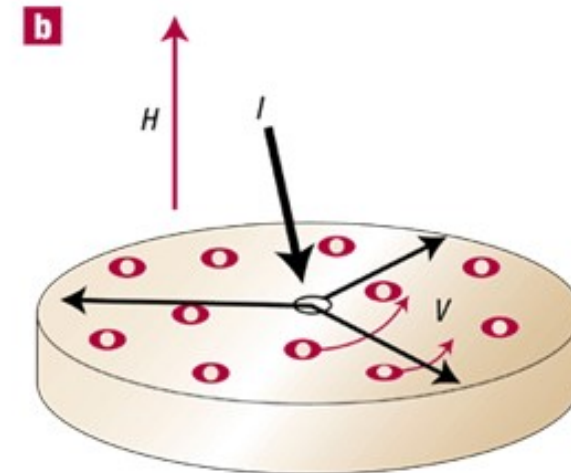
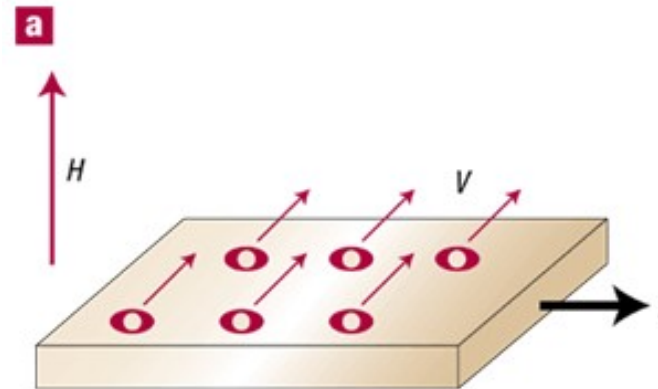


random injection of
the disordered phase

random annealing
by the current flow



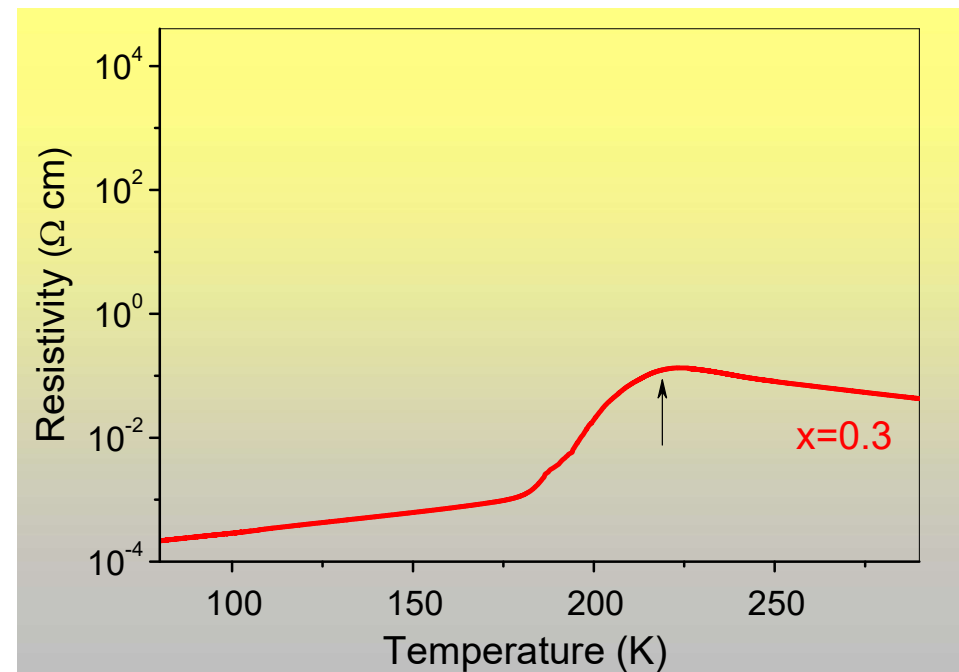
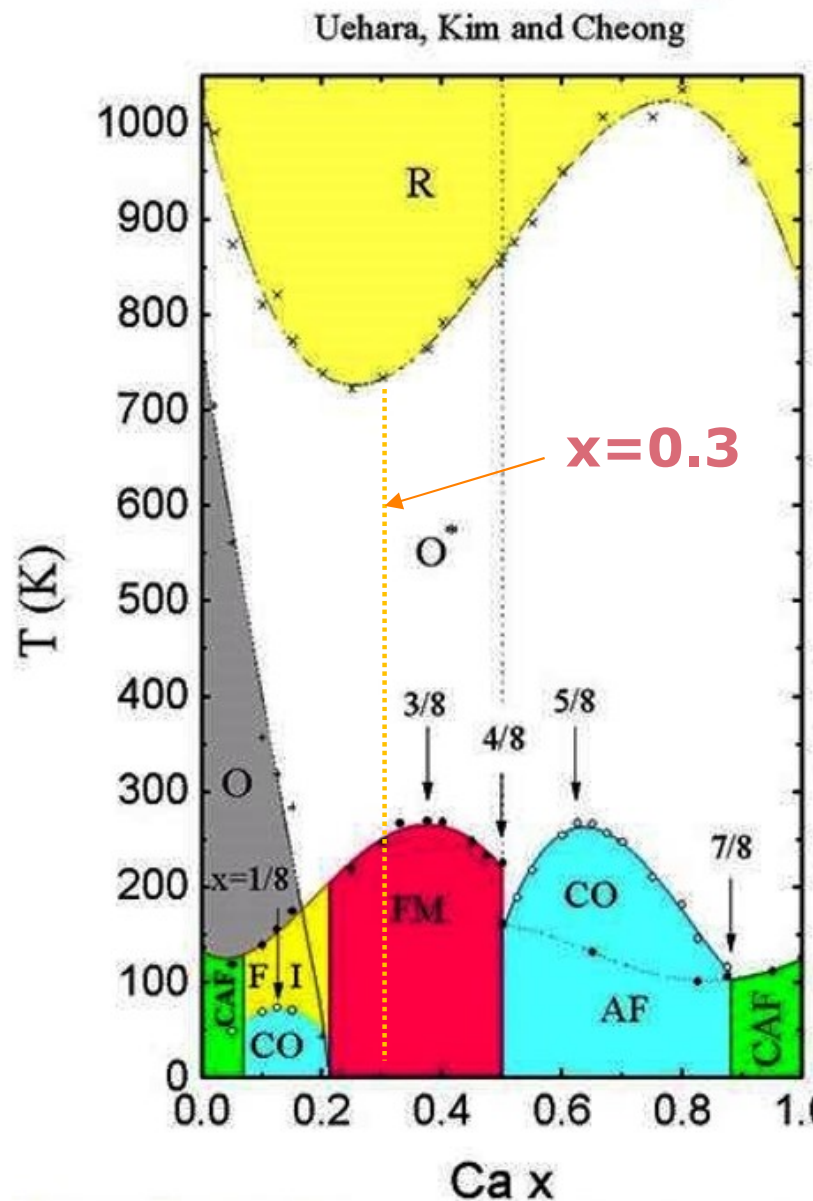
Corbino disk – mechanism verification



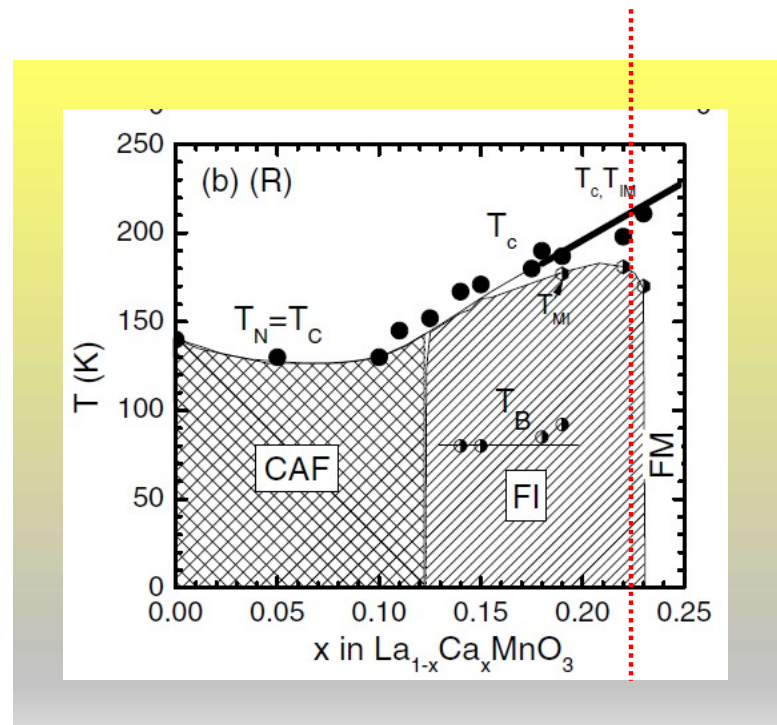
M-RTN in manganites

- M-RTN in mixed valance manganites exhibiting Colossal Magneto-Resistive (CMR) effect is typically ascribed to two mechanisms:
 - Pronounced phase separation (PS) resulting in coexistence of percolating paths with significantly different conductivity (most pronounced near M-I or CO transitions).
 - Fluctuations of magnetic moments which couple to the resistivity noise through CMR effect (most pronounced near PM-FM transition).
- Such M-RTN manifestations are typically limited to relatively narrow temperature ranges and are characterized by strong dependence of RTN switching rates on applied magnetic field and current bias.
- Recently we have observed yet another peculiar type of M-RTN in the conductivity of low doped $\text{La}_x\text{Ca}_{1-x}\text{MnO}_3$ manganite single crystals. Robust M-RTN appears in a very wide temperature range and is characterized by completely magnetic field and bias independent switching rates.

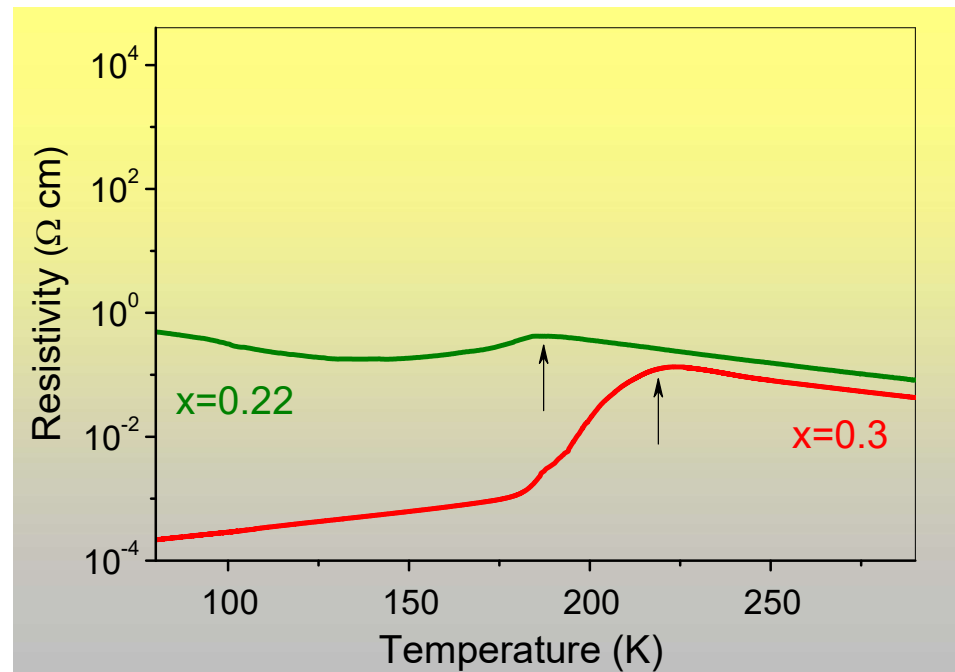
$\text{La}_{1-x}\text{Ca}_x\text{MnO}_3$: Low Ca-doping



$\text{La}_{1-x}\text{Ca}_x\text{MnO}_3$: Low Ca-doping



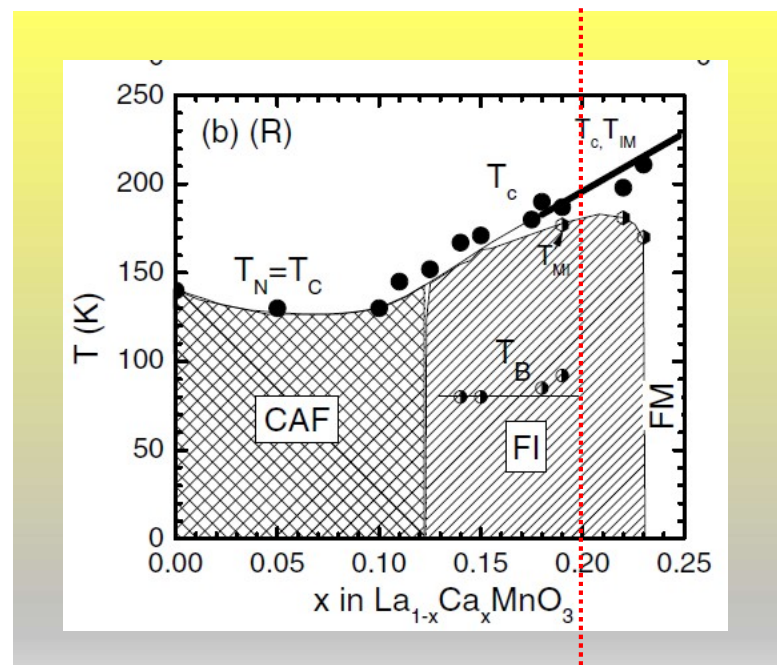
$x=0.22$



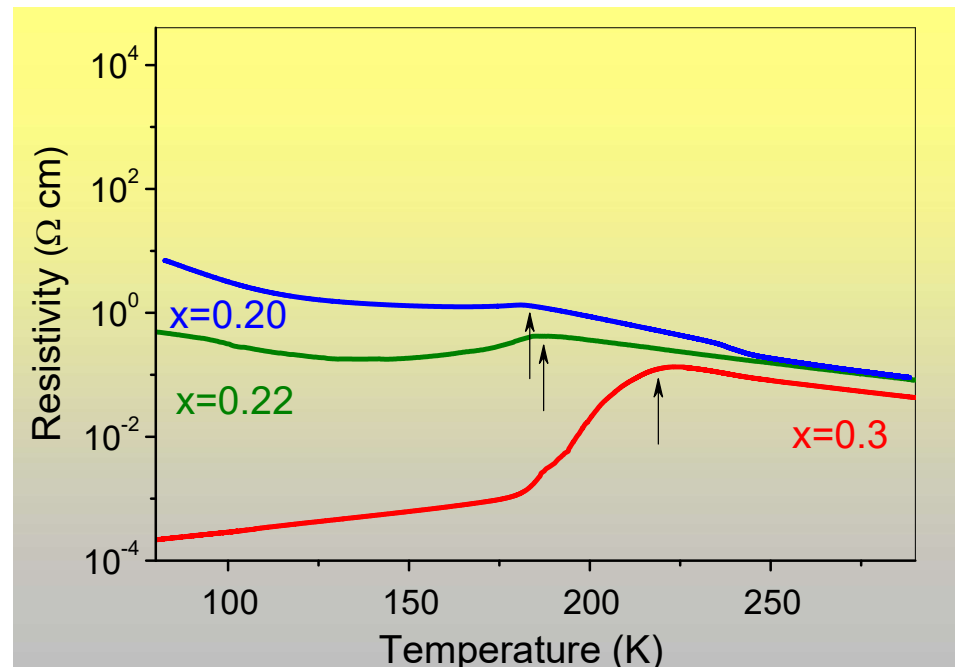
Phase diagram from:

M. Pissas and G. Papavassiliou, J. Phys.: Condens. Matter 16 (2004) 6527–6540

$\text{La}_{1-x}\text{Ca}_x\text{MnO}_3$: Low Ca-doping



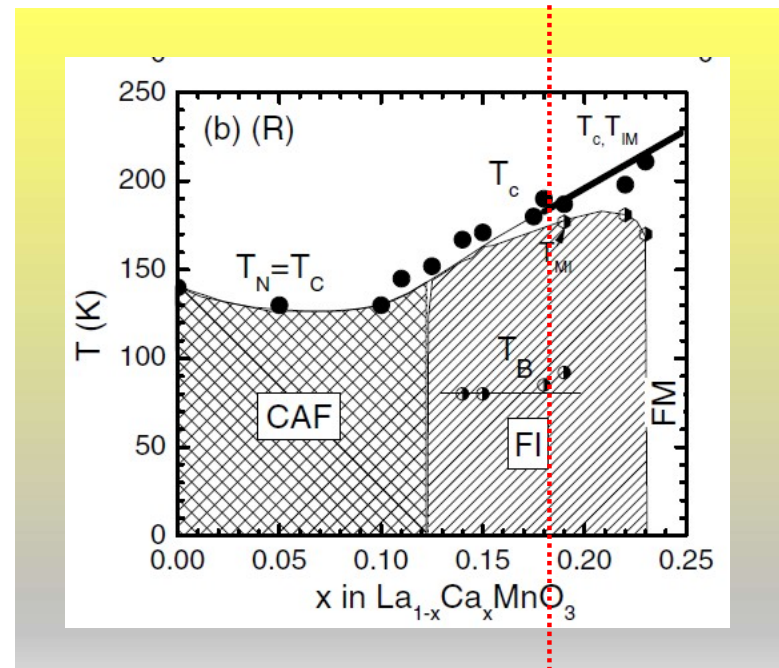
$x=0.20$



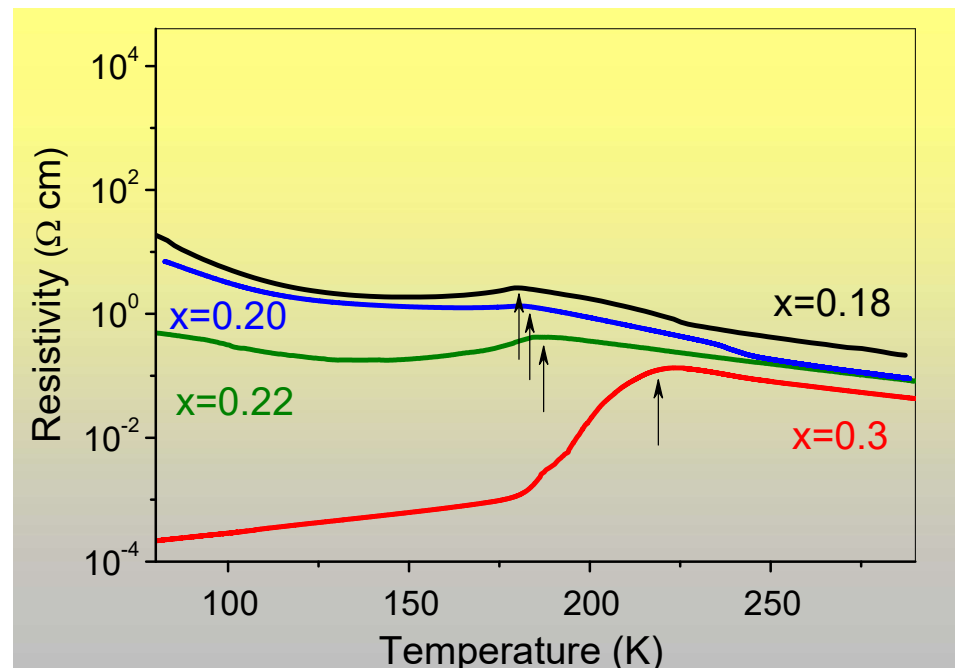
Phase diagram from:

M. Pissas and G. Papavassiliou, J. Phys.: Condens. Matter 16 (2004) 6527–6540

$\text{La}_{1-x}\text{Ca}_x\text{MnO}_3$: Low Ca-doping



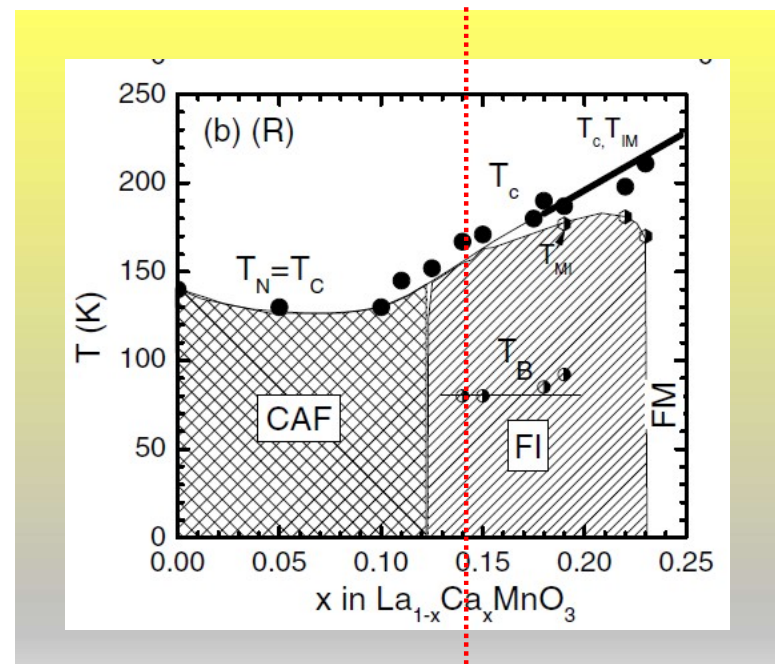
$x=0.18$



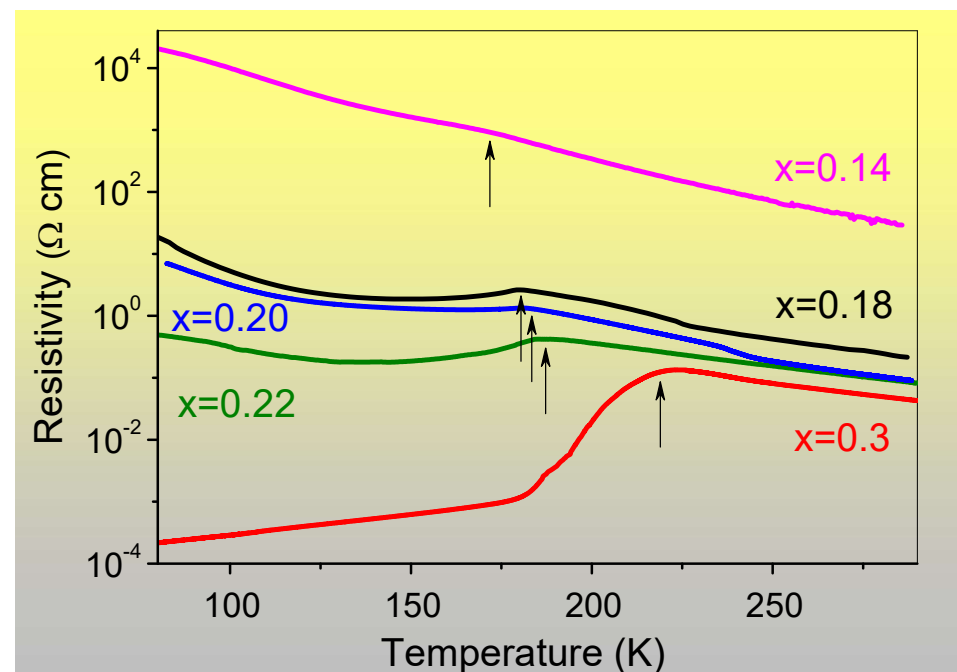
Phase diagram from:

M. Pissas and G. Papavassiliou, J. Phys.: Condens. Matter 16 (2004) 6527–6540

$\text{La}_{1-x}\text{Ca}_x\text{MnO}_3$: Low Ca-doping



x=0.14



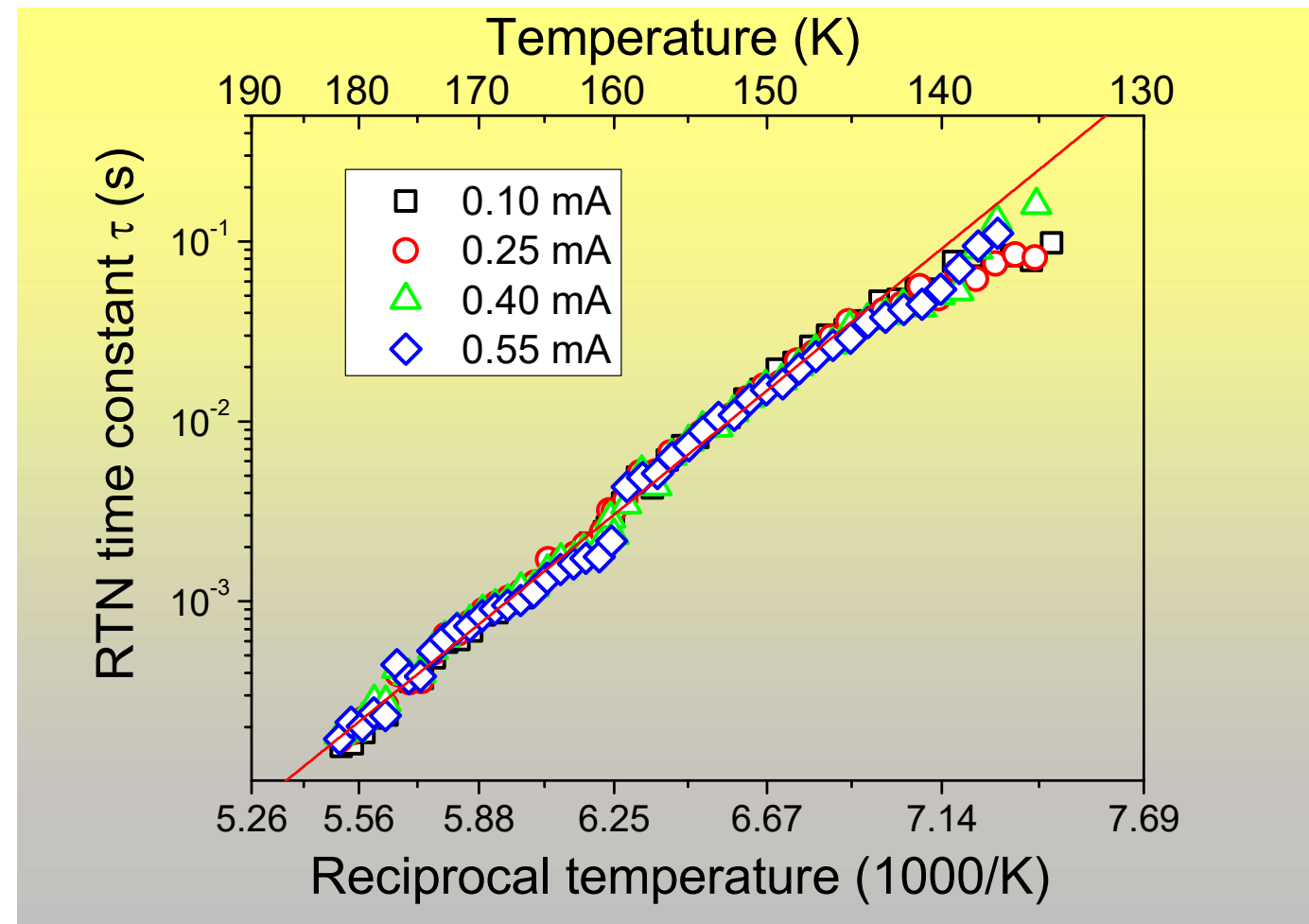
Phase diagram from:

M. Pissas and G. Papavassiliou, J. Phys.: Condens. Matter 16 (2004) 6527–6540

Robust M-RTN: switching rate

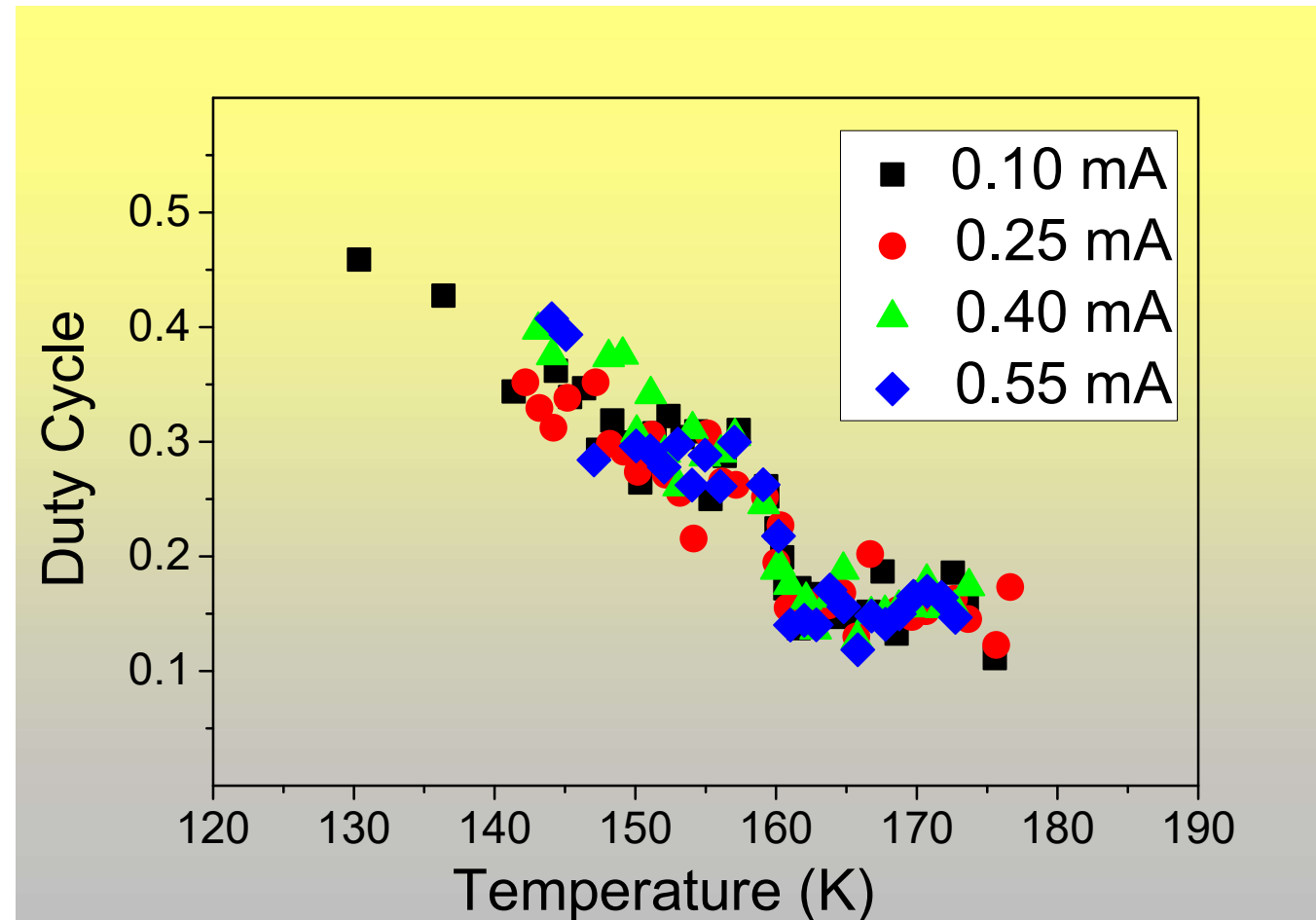
$$\tau = \frac{\tau_{up}\tau_{dn}}{\tau_{up} + \tau_{dn}}$$

La_{0.86}Ca_{0.14}MnO₃ single crystal

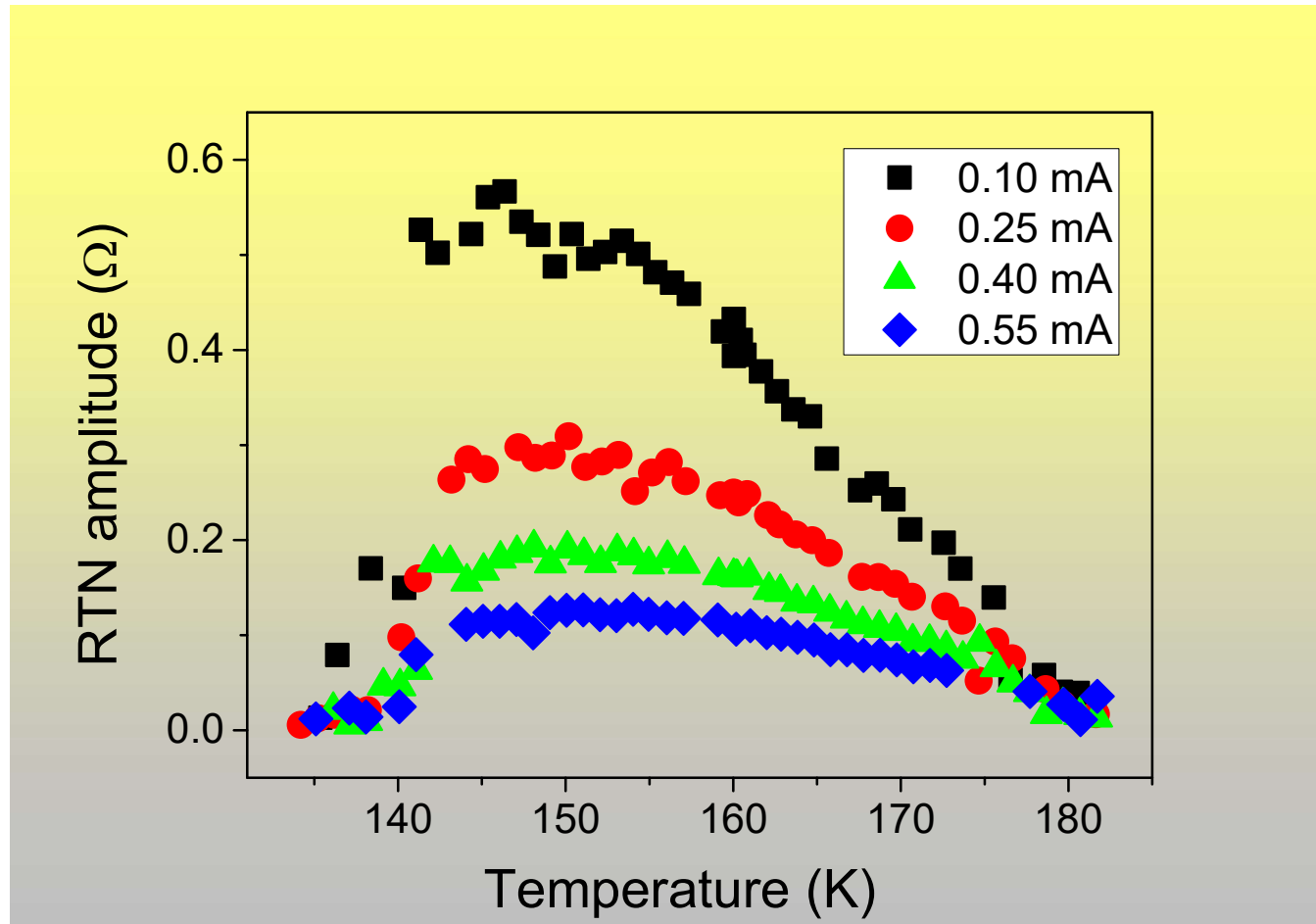


Robust M-RTN: duty cycle

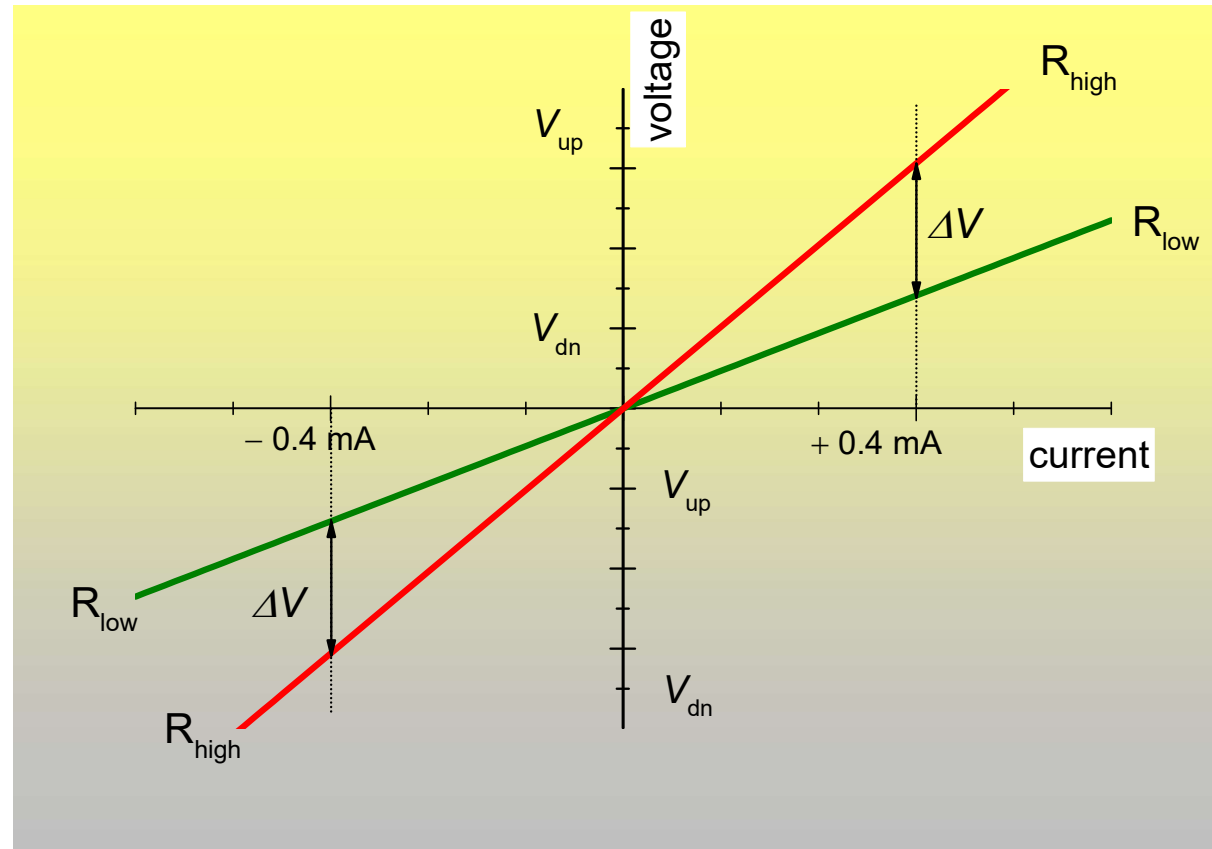
$$D = \frac{\tau_{up}}{\tau_{up} + \tau_{dn}}$$



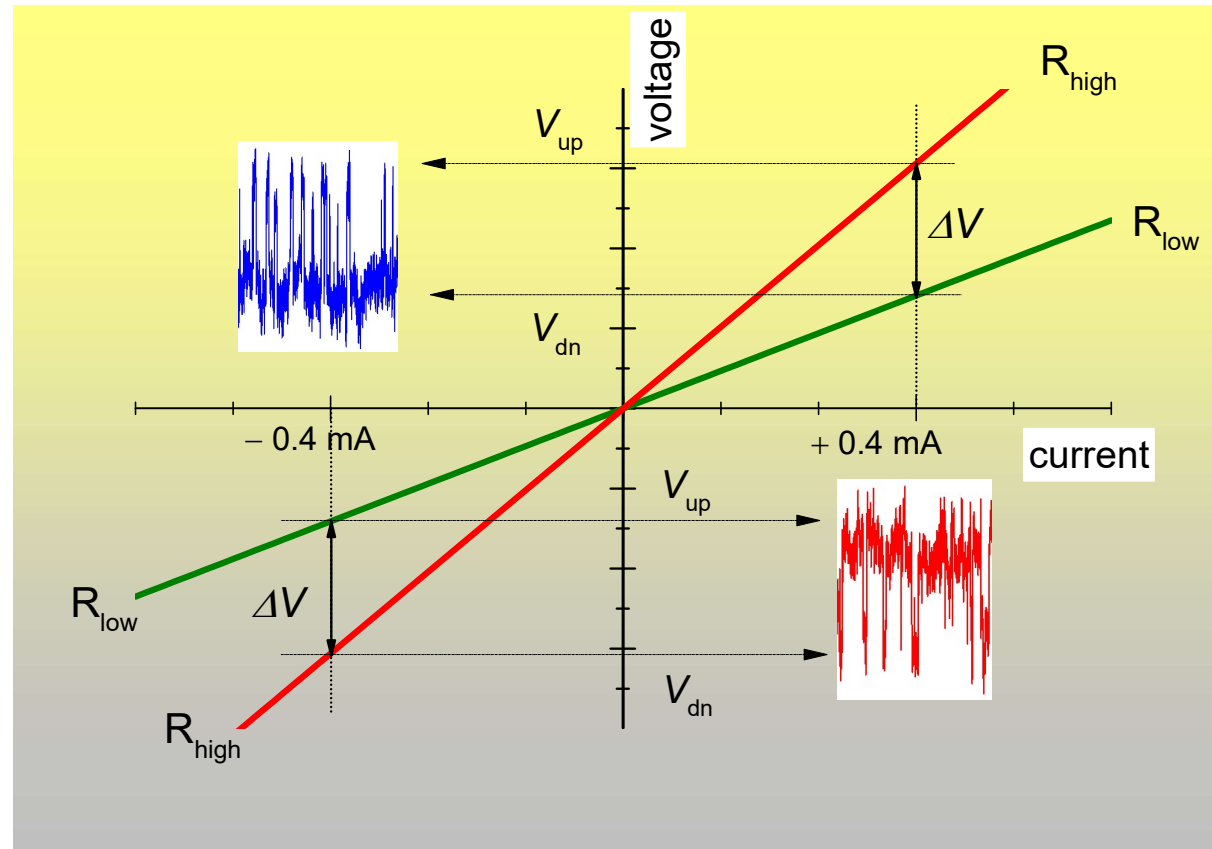
Robust M-RTN: amplitude



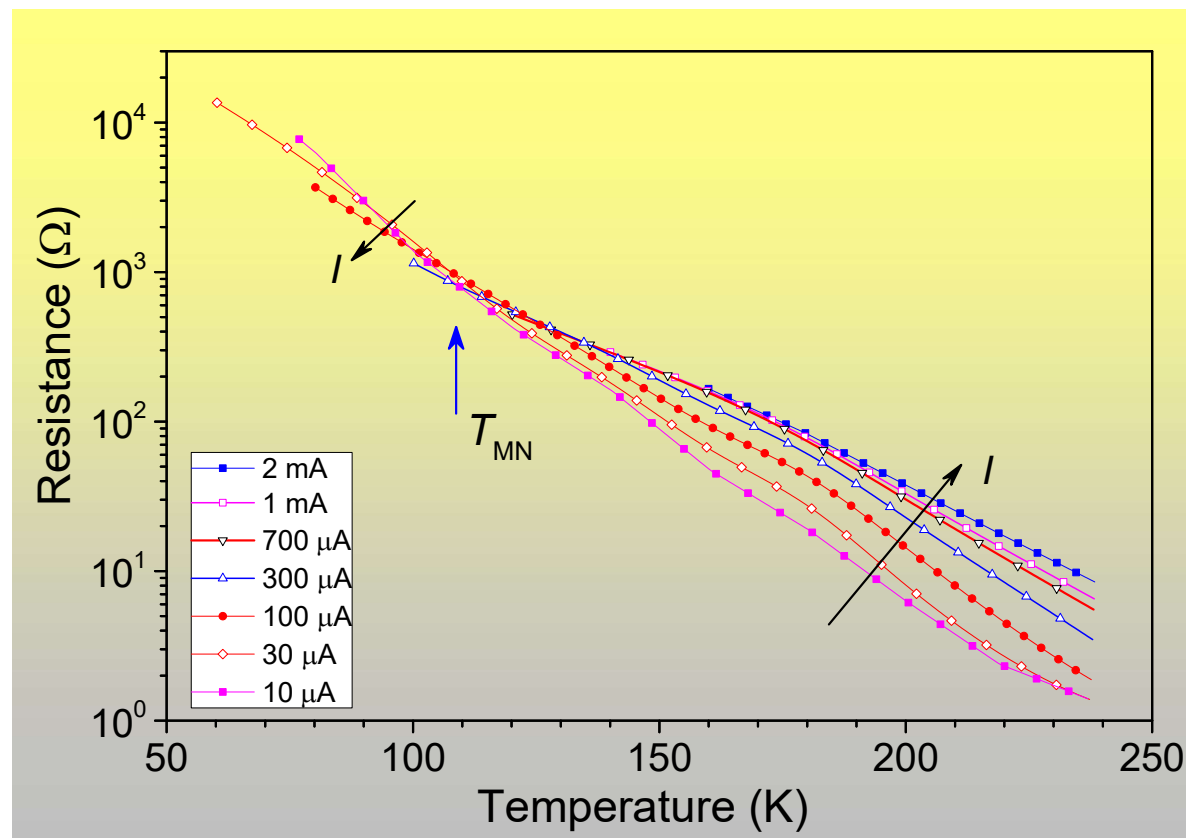
M-RTN due to resistivity fluctuations



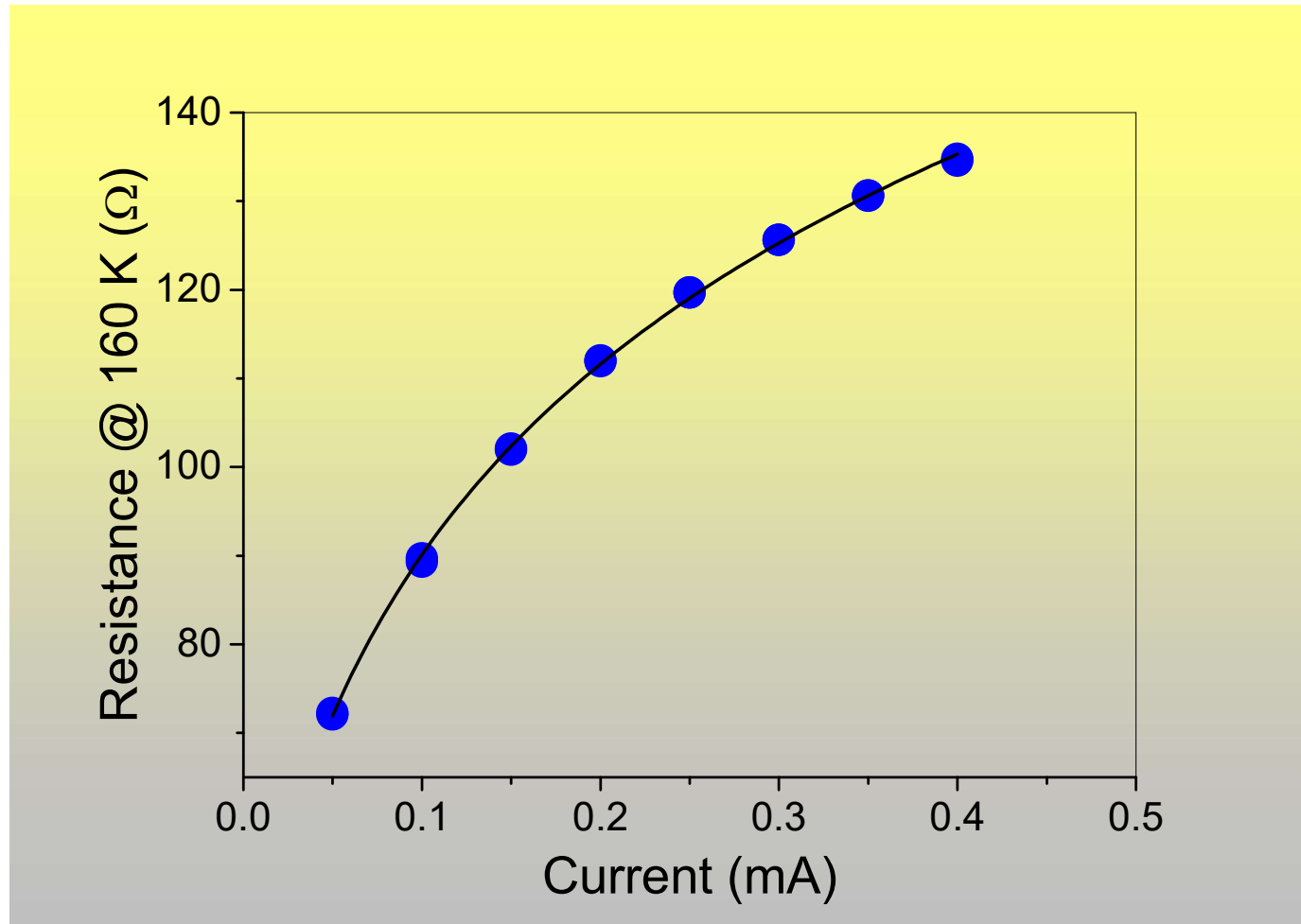
M-RTN due to resistivity fluctuations



$R(T,I)$ La_{0.86}Ca_{0.14}MnO₃ single crystal



$R(I)$ @ 160 K



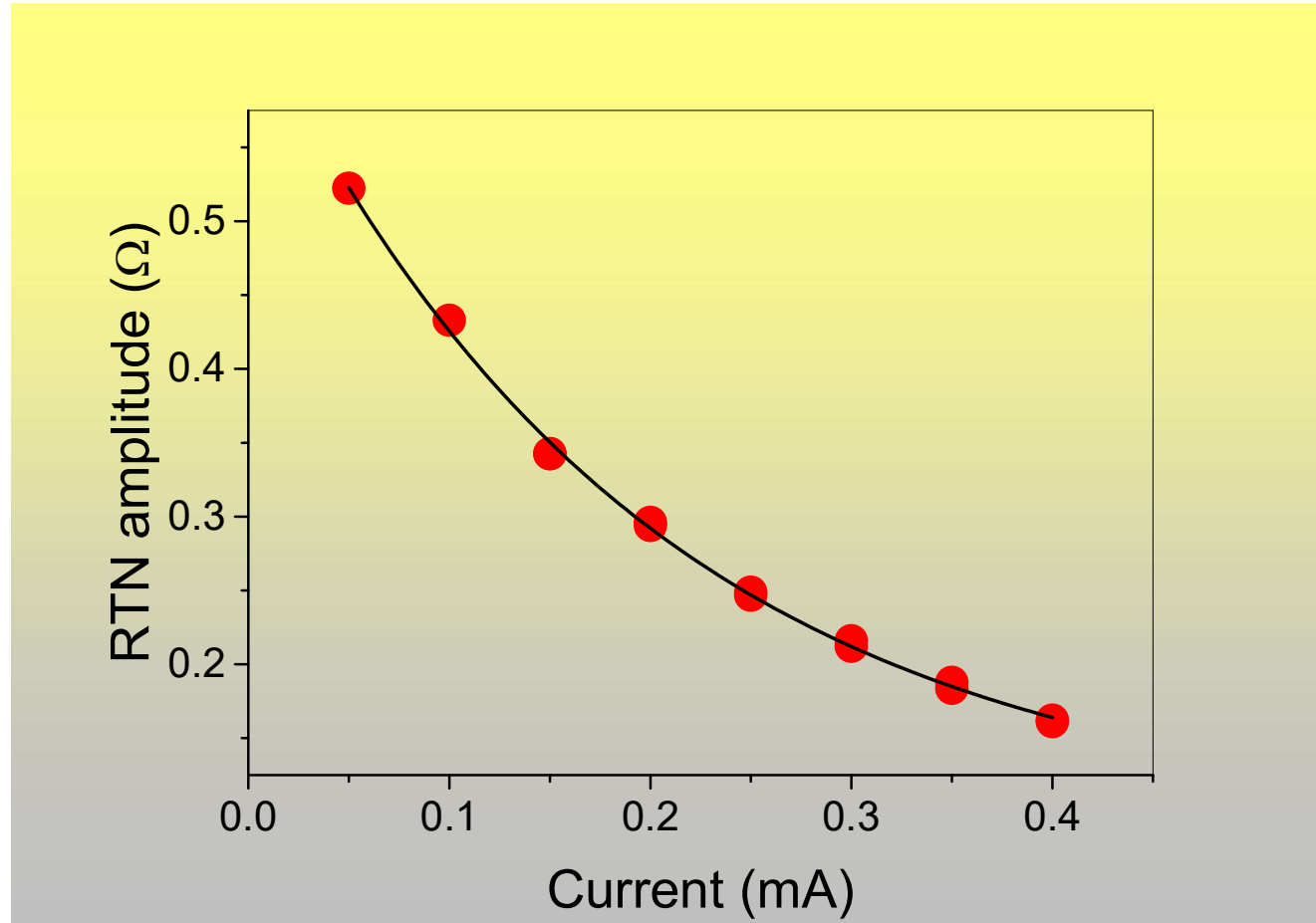
$$R = a + b e^{-kI}$$

$$a = 147.2 \pm 0.6$$

$$b = -98.2 \pm 0.4$$

$$k = 5020 \pm 80$$

M-RTN amplitude: current dependence



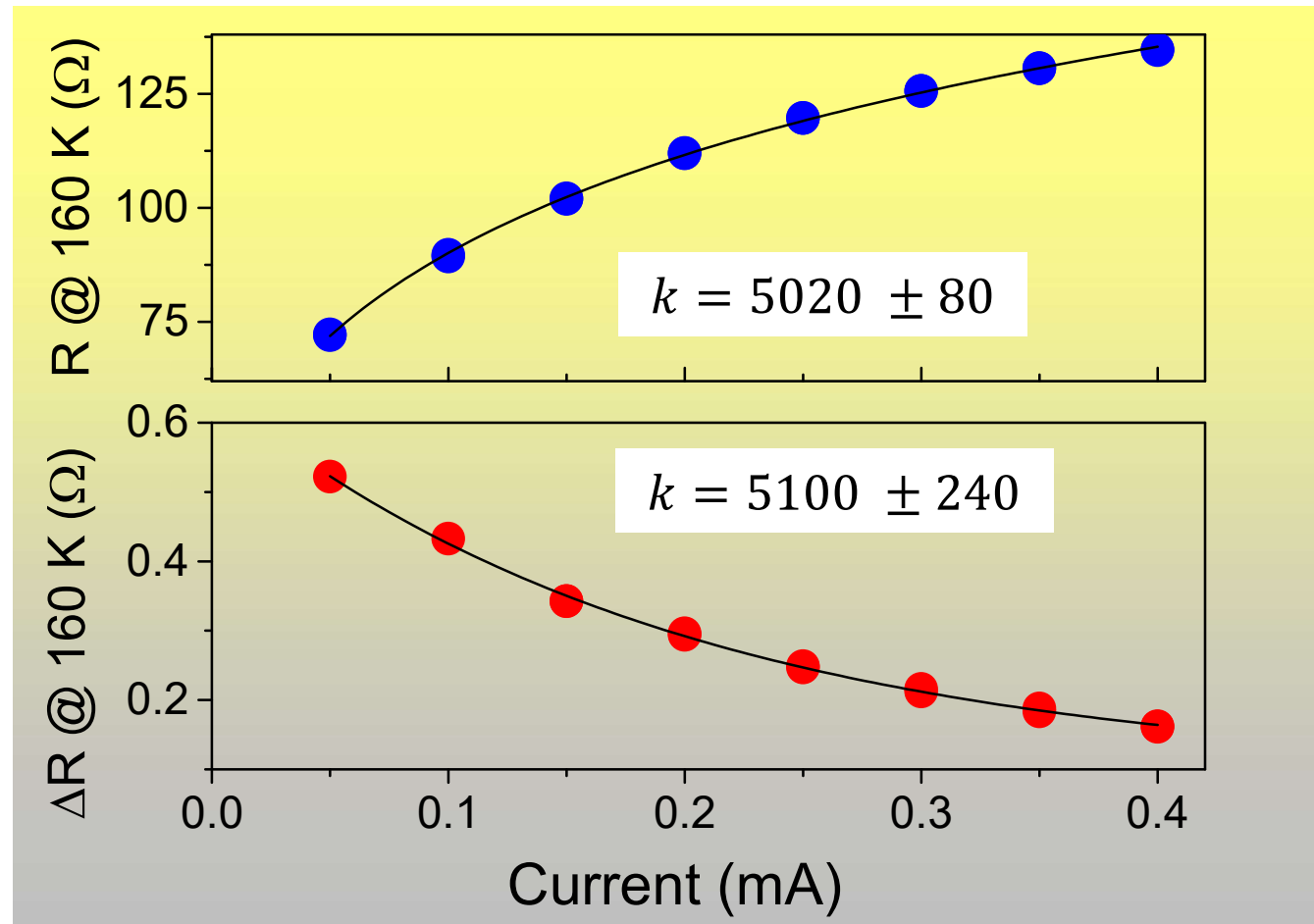
$$\Delta R = a + b e^{-kI}$$

$$a = 0.092 \pm 0.009$$

$$b = 0.556 \pm 0.007$$

$$k = 5100 \pm 240$$

Exponential dependence on current

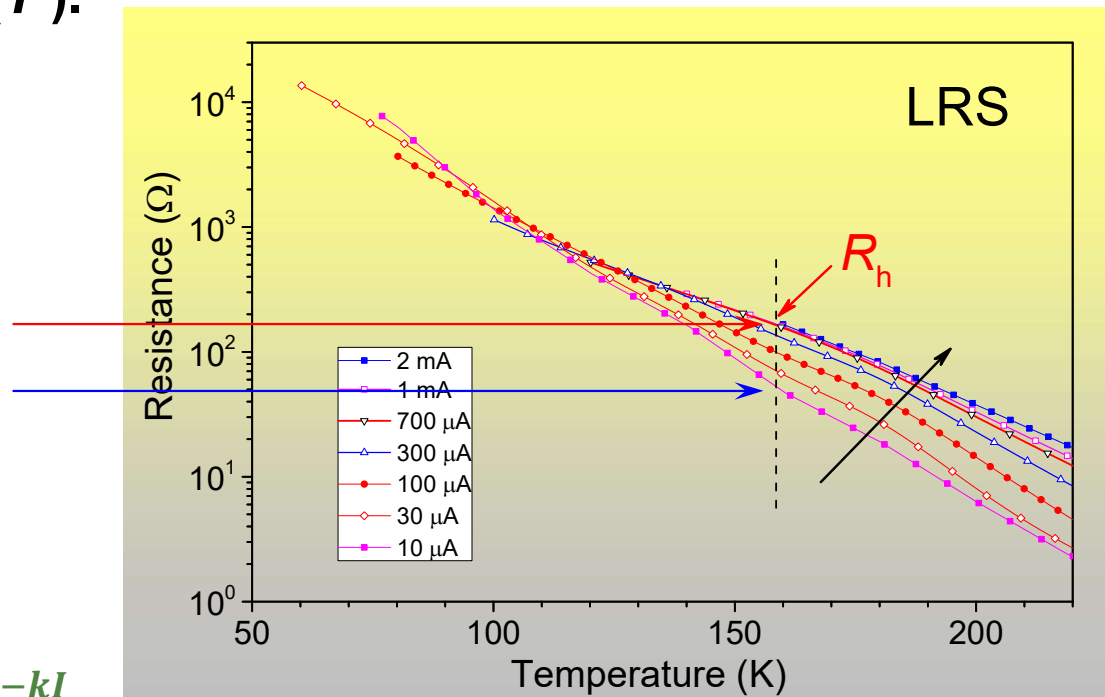


$$y = a + b e^{-kI}$$

RTN toy model

RTN consists in switching of a fraction β of the total sample resistance between current-dependent resistivity $R(T,I)$ and current-independent, saturated high resistivity $R_h(T)$.

$$\Delta R(I,T) = \beta [R_h(T) - R(I,T)]$$

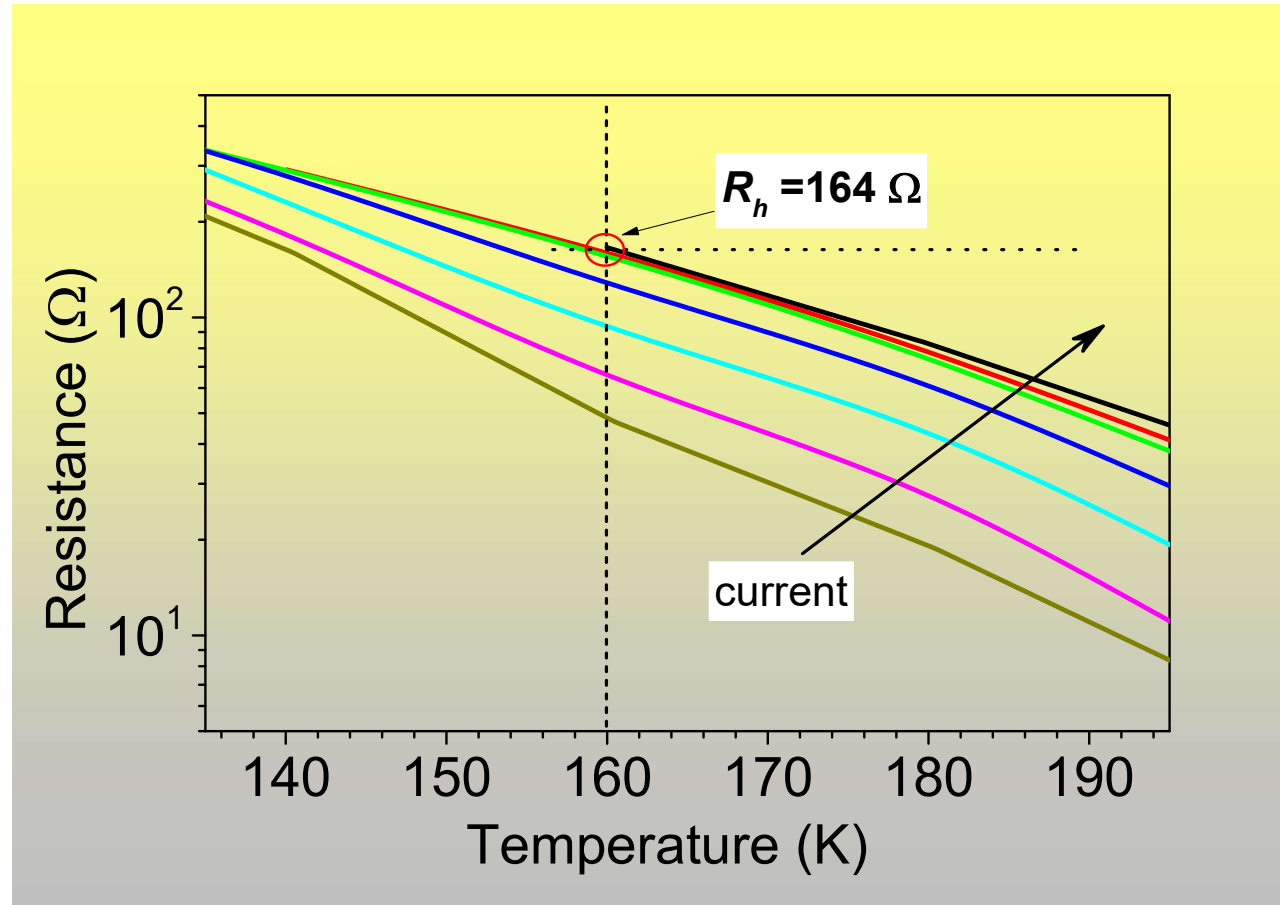


$$\left\{ \begin{array}{l} \Delta R(I@160K) = 0.09 + 0.556 e^{-kI} \\ \Delta R(I@160K) = \beta [R_h(160 K) - (147 - 98.2 e^{-kI})] \end{array} \right.$$

$$\beta (160 K) = 5.7 \times 10^{-3} \rightarrow V_{TLF} = \beta V_s = 5.7 \times 10^{-12} m^3, \quad V_s = 10^{-9} m^3$$

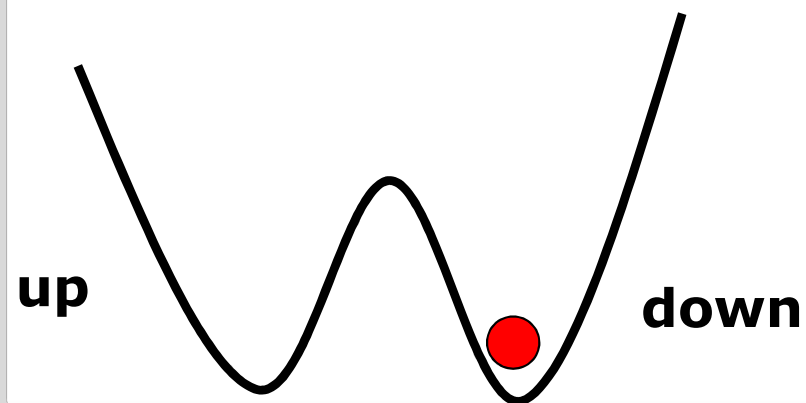
$$R_h(160 K) = 162.5 \Omega$$

Saturated resistance @160 K verification

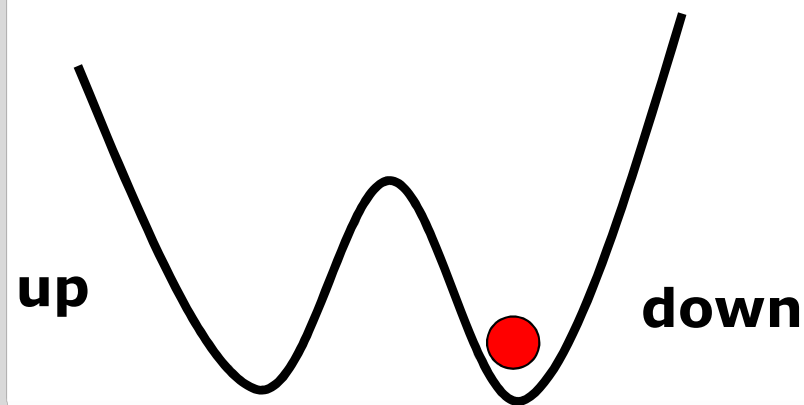
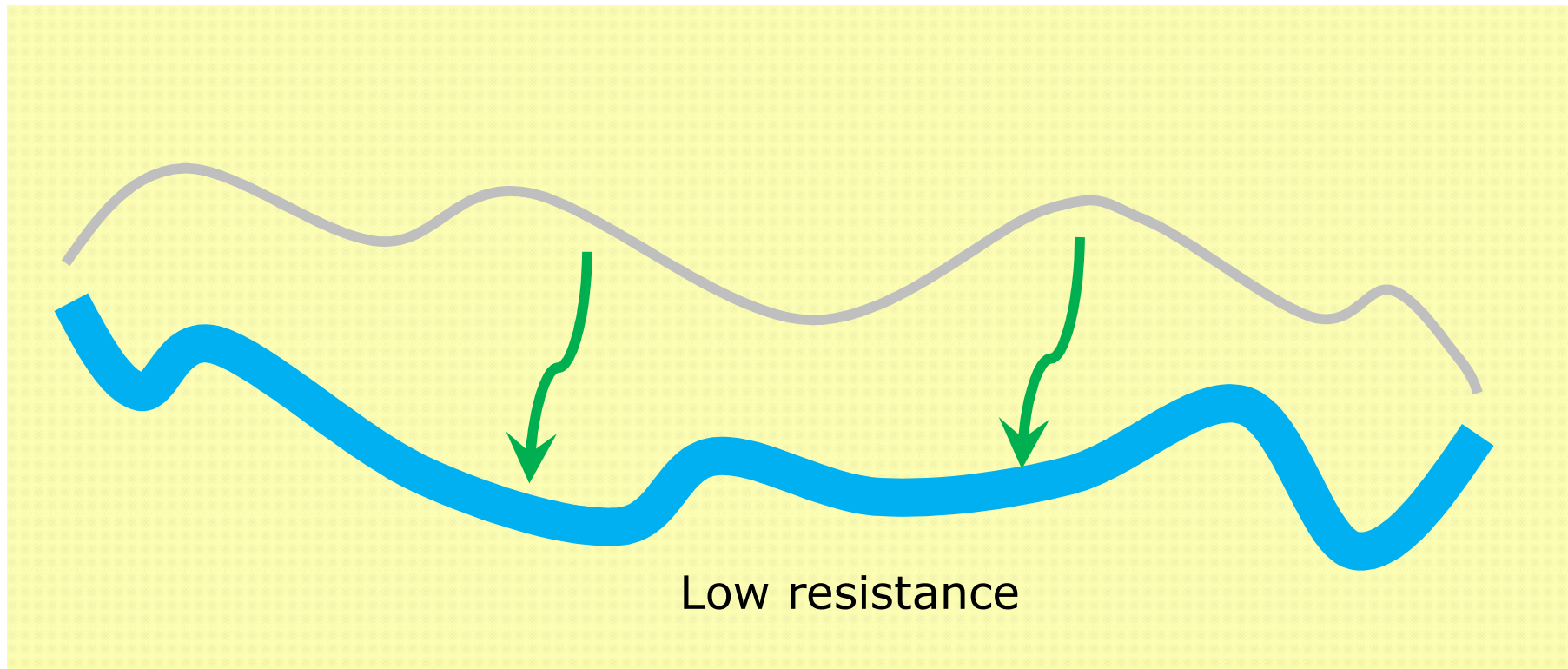


$$R_h(\text{model}) = 162.5 \Omega$$

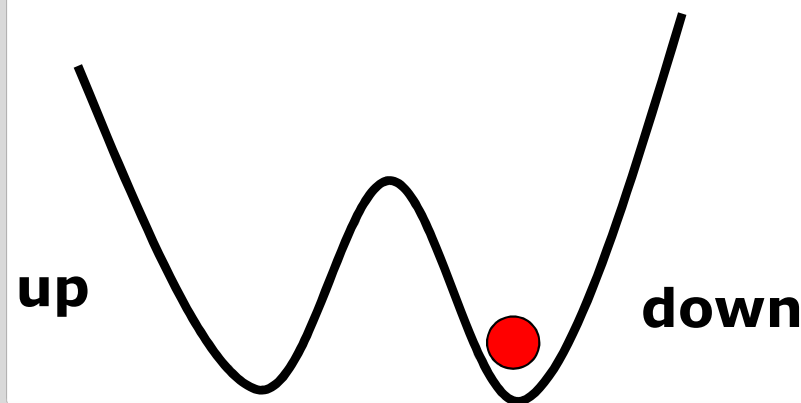
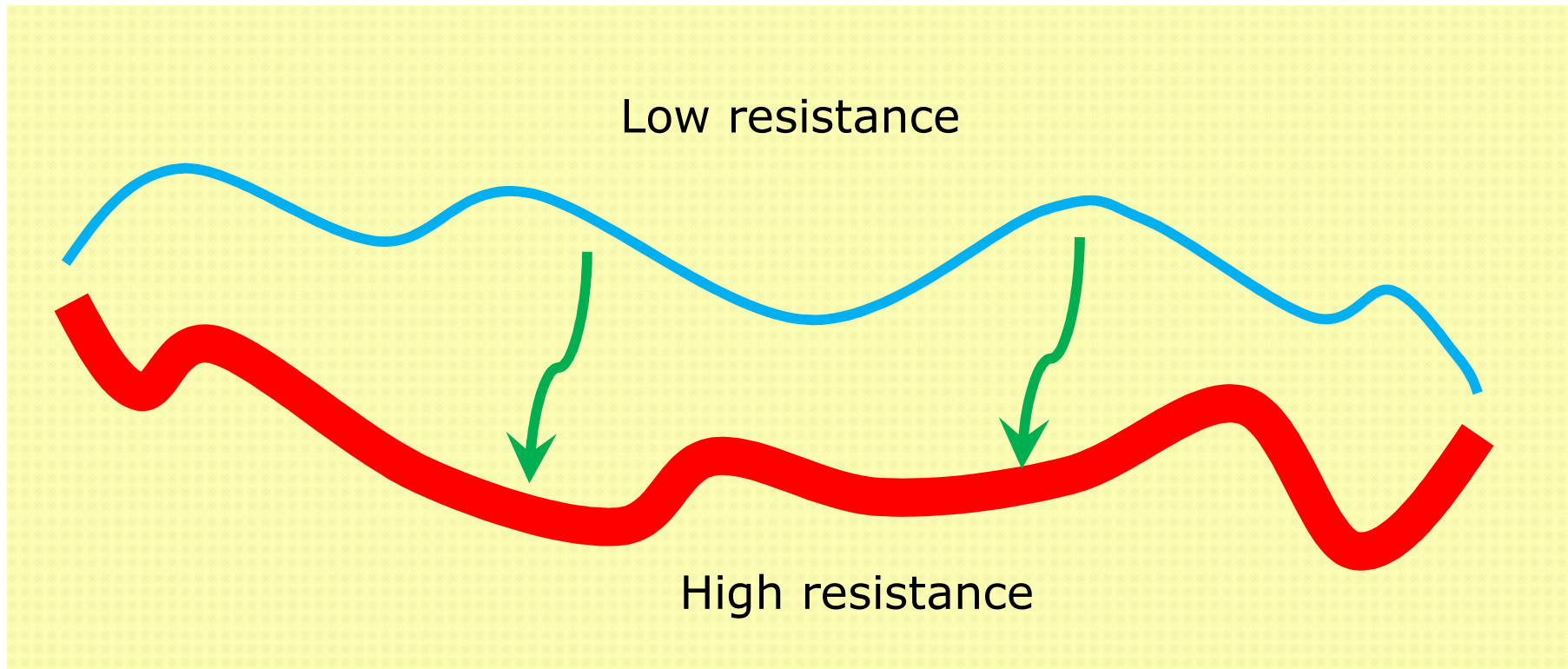
Dynamic current redistribution as TLF



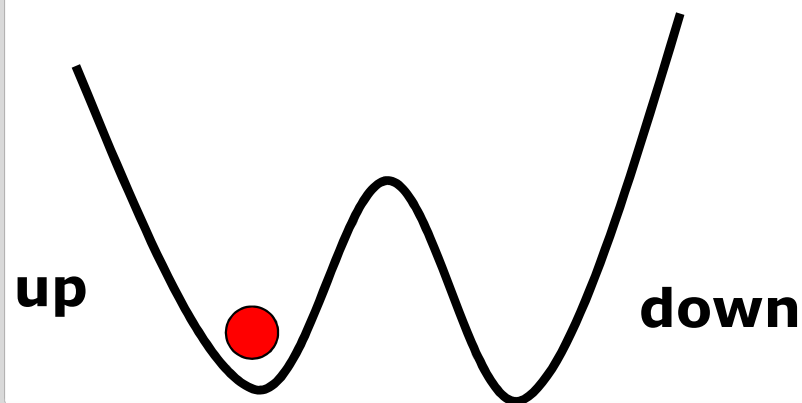
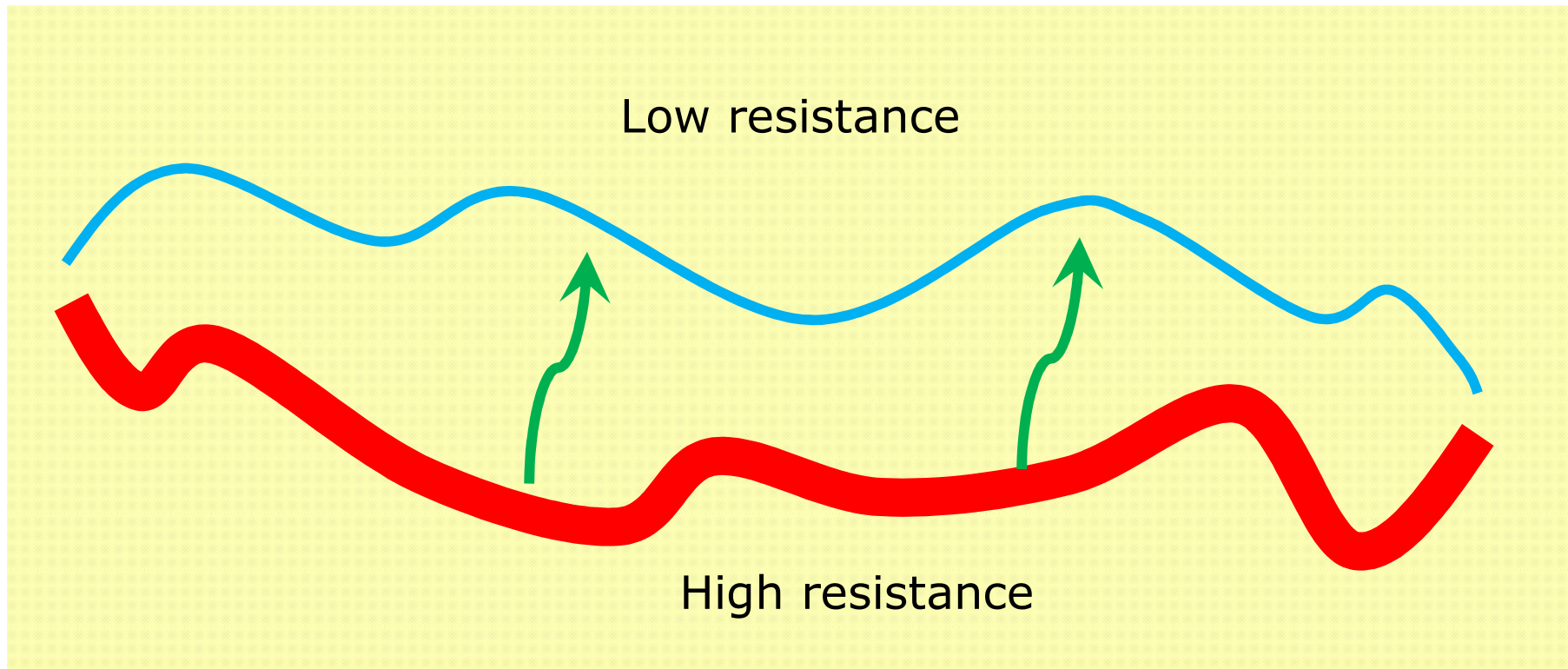
Dynamic current redistribution as TLF



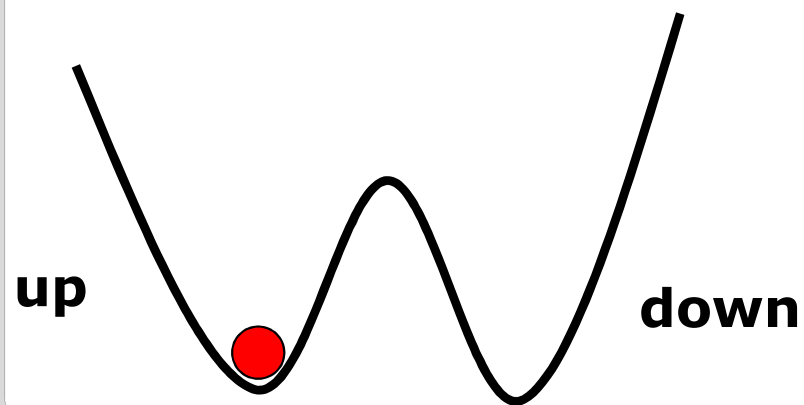
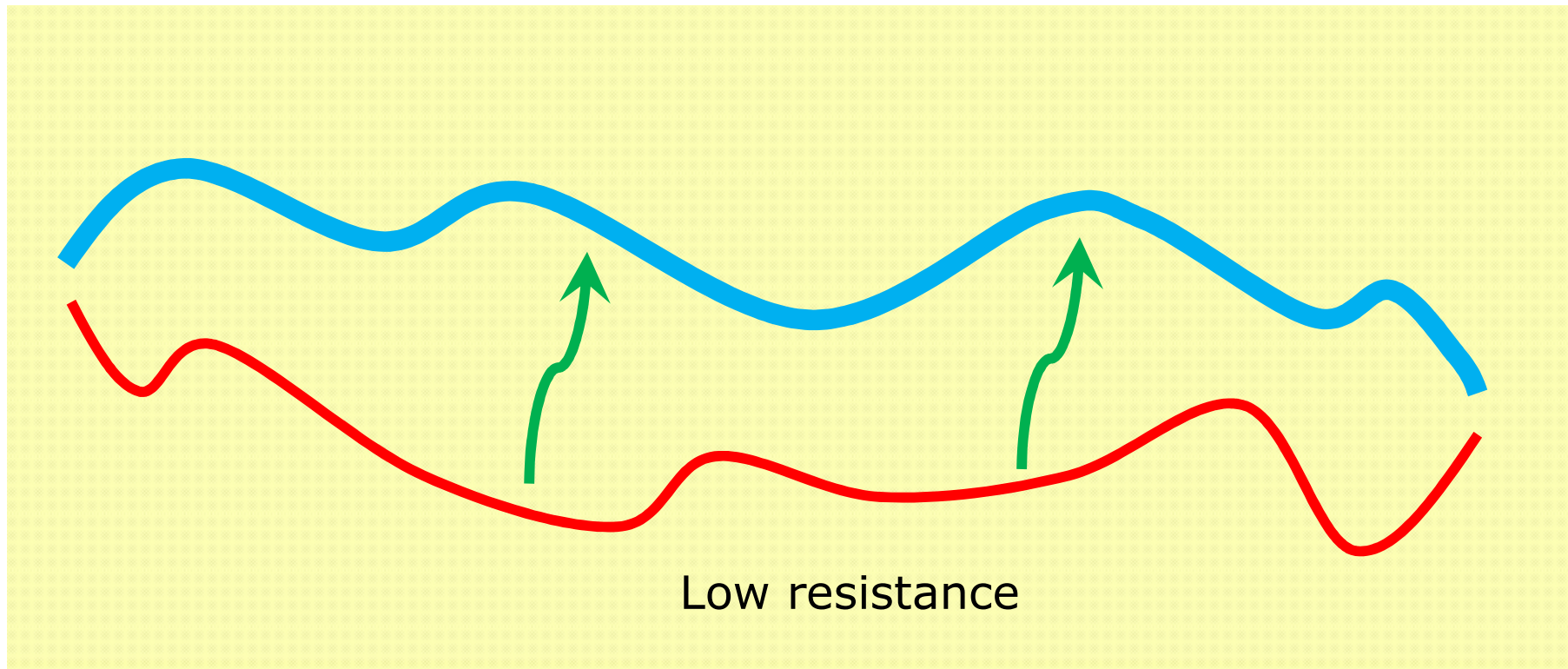
Dynamic current redistribution as TLF



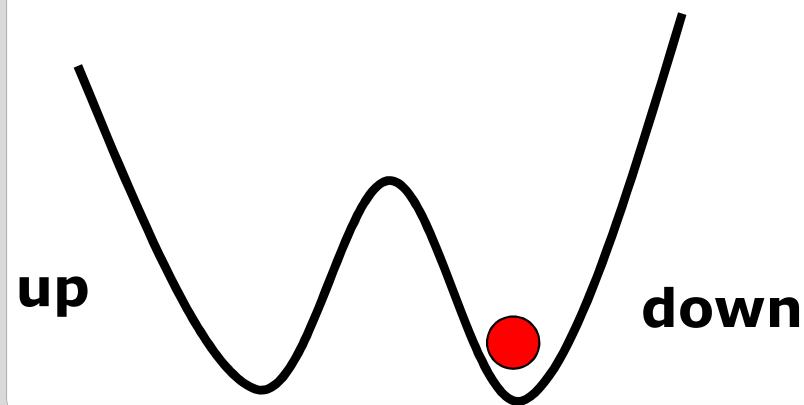
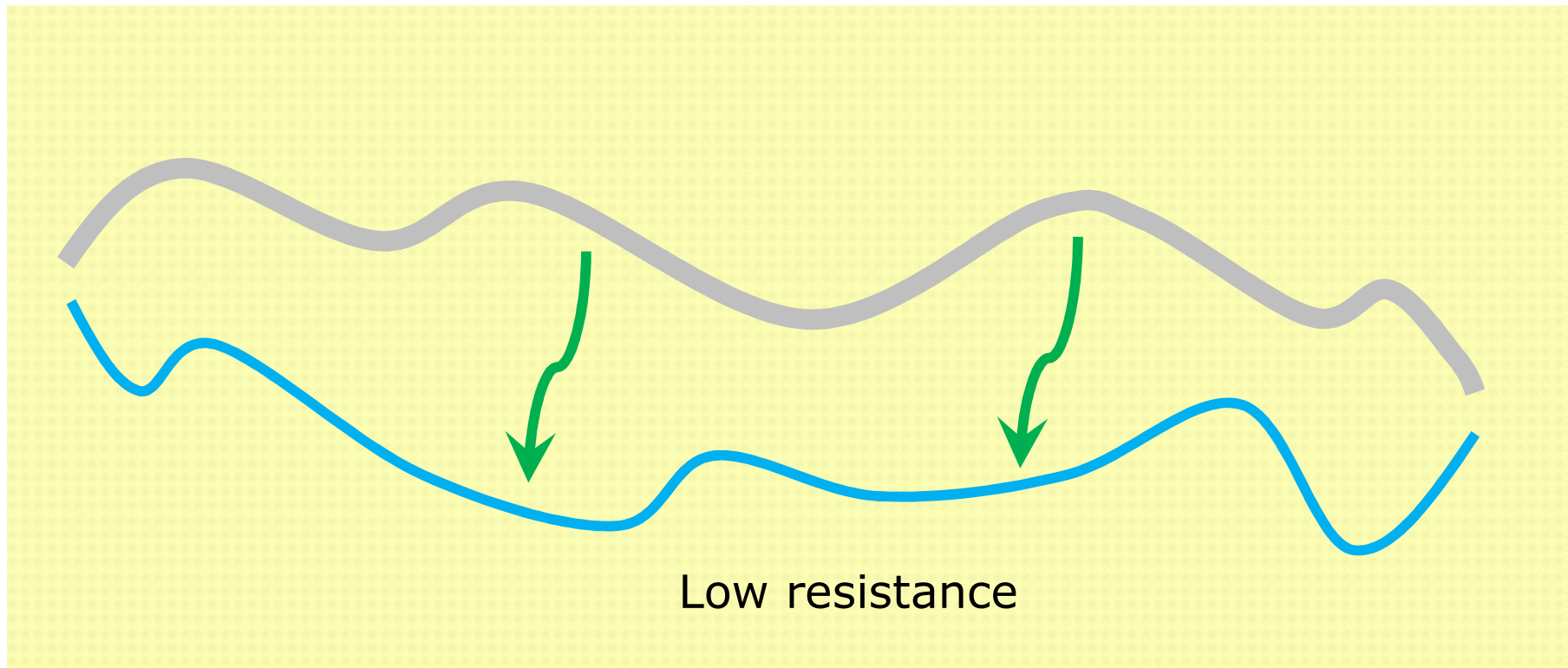
Dynamic current redistribution as TLF



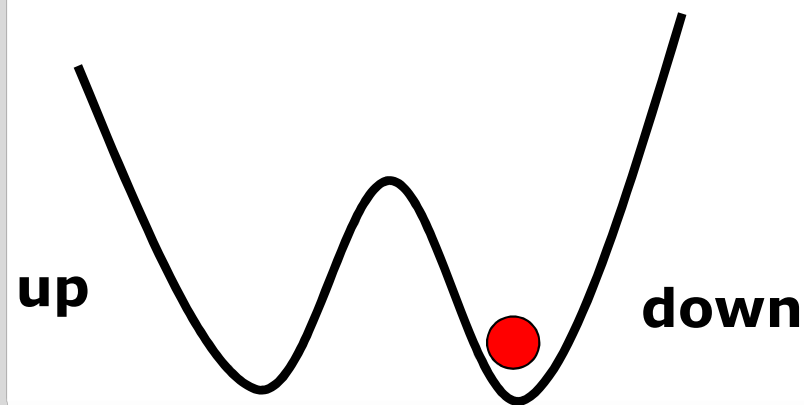
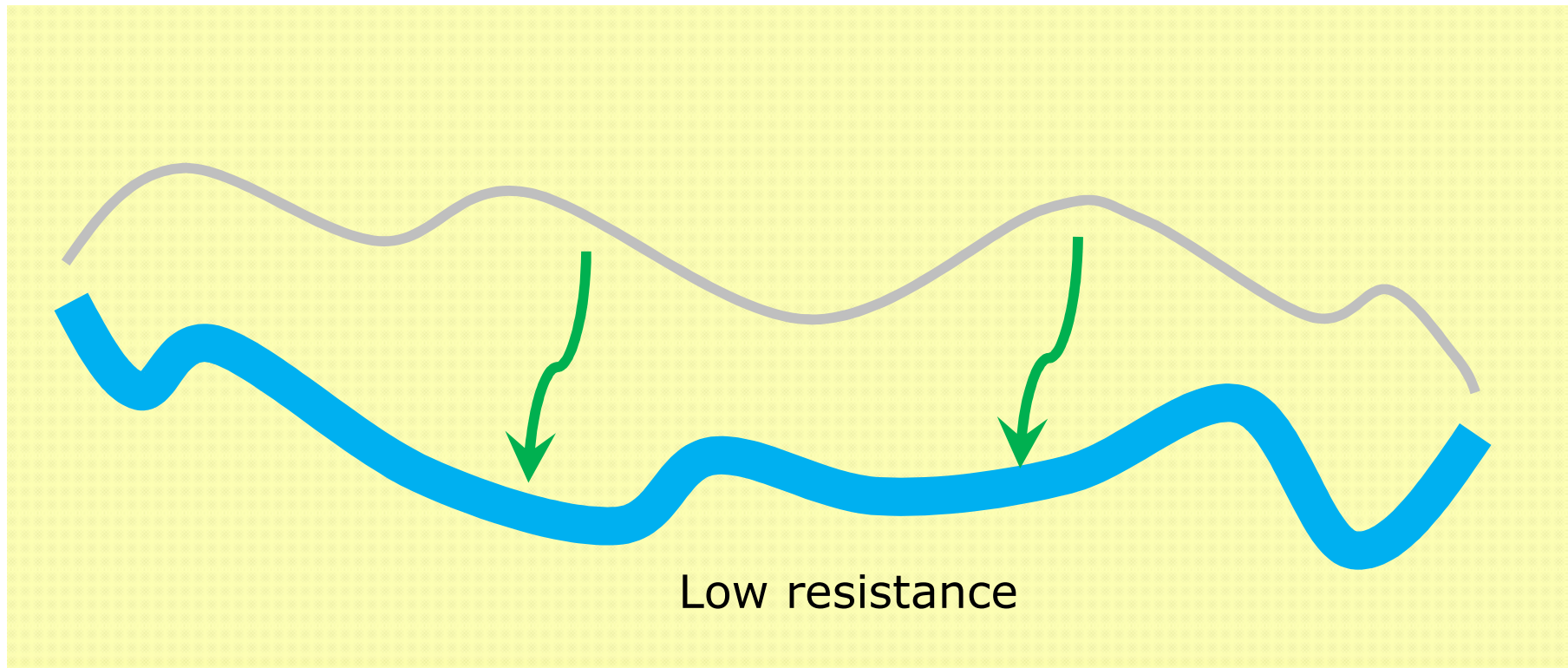
Dynamic current redistribution as TLF



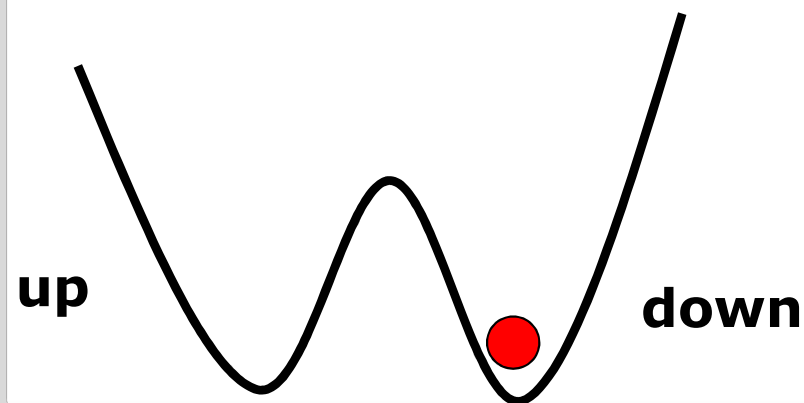
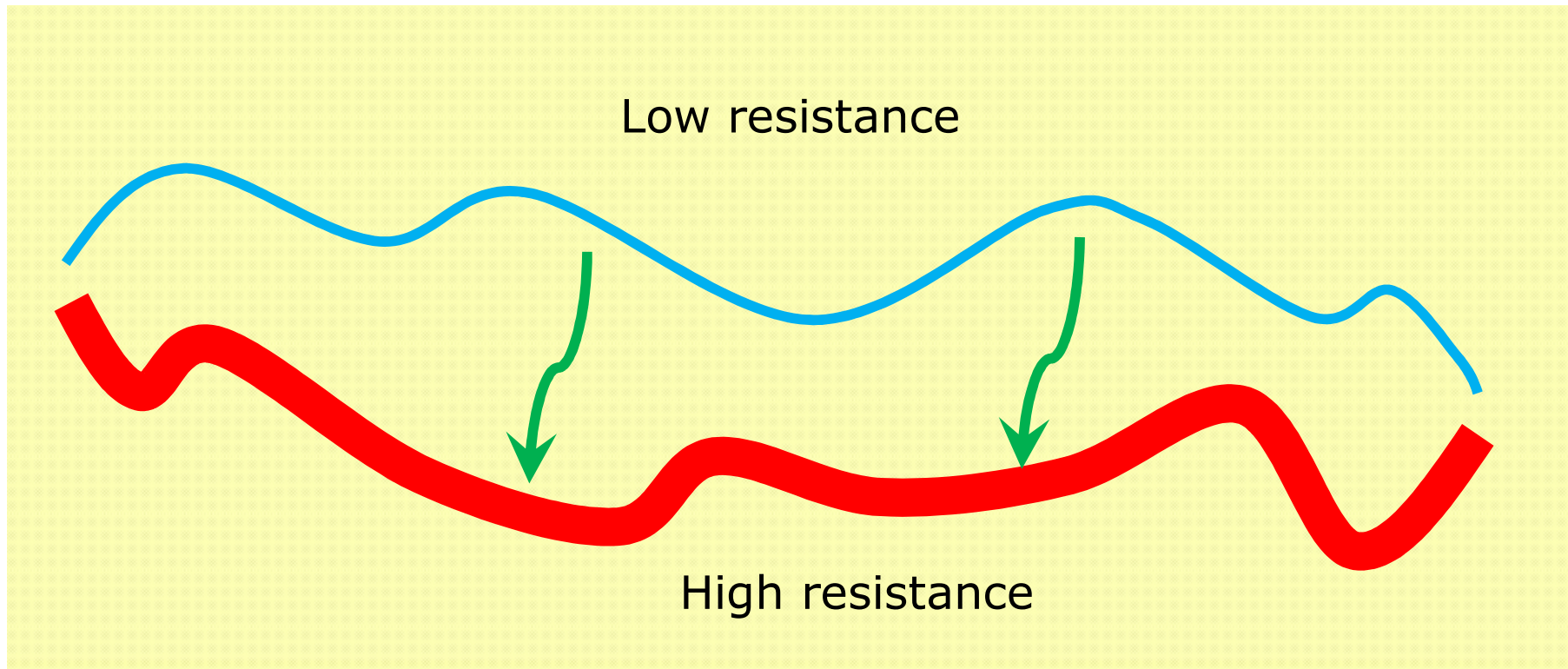
Dynamic current redistribution as TLF



Dynamic current redistribution as TLF



Dynamic current redistribution as TLF



M-RTN Feedback mechanism

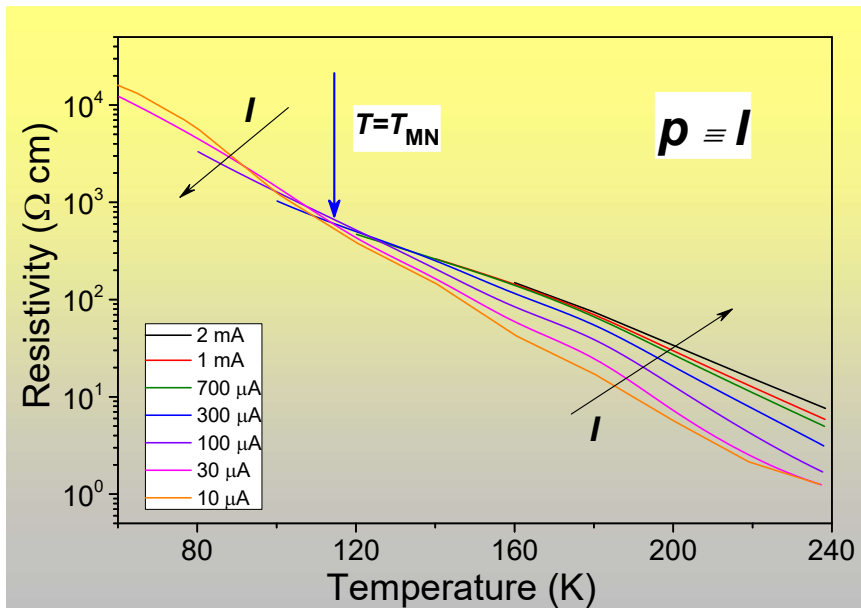
Thermally activated resistivity

$$\rho(T) = \rho_0 \exp\left(-\frac{E_a}{k_B T}\right)$$

Meyer-Neldel Rule*

$$\rho(T) = \rho_{00} \exp\left(\frac{E_a}{k_B T_{MN}}\right) \exp\left(-\frac{E_a}{k_B T}\right)$$

*) Original paper: W. Meyer and H. Neldel, Z. Techn. **18**, 588 (1937)



$E_a = E_a(p)$ then $\rho = \rho(p)$;

@ $T = T_{MN}$ $\rho \neq \rho(p)$

$$G = H - TS$$

$$\rho(T) = \rho_0 \exp\left(-\frac{\Delta G}{k_B T}\right) = \rho_{00} \exp\left(\frac{\Delta S}{k_B}\right) \exp\left(-\frac{\Delta H}{k_B T}\right)$$

Multiple excitations entropy model

Large activation barrier $\Delta H \gg \hbar\omega_0$

$$n = \frac{\Delta H}{\hbar\omega_0} \quad \text{excitations out of } N \text{ available excitations in the interaction volume}$$

$$\Delta S = k_B \ln W = k_B \ln \frac{N!}{n!(N-n)!}$$

For $N \gg n$, using Stirling's approximation,

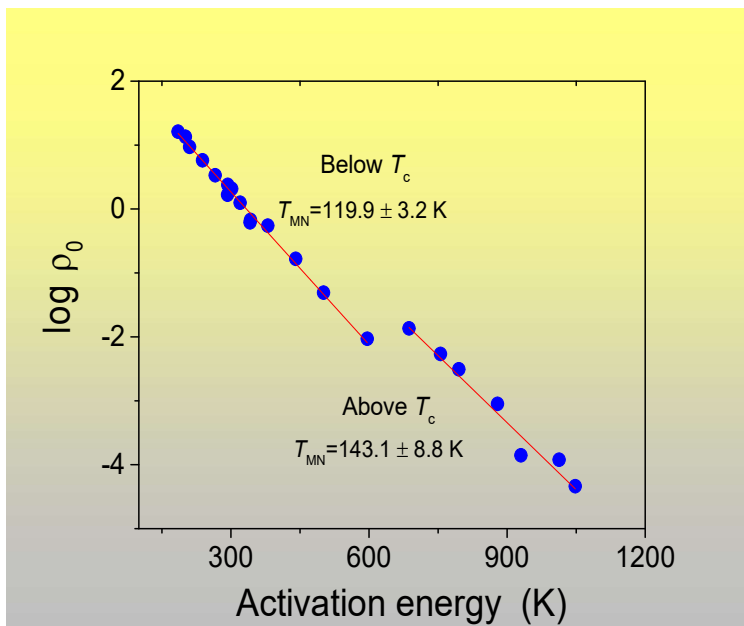
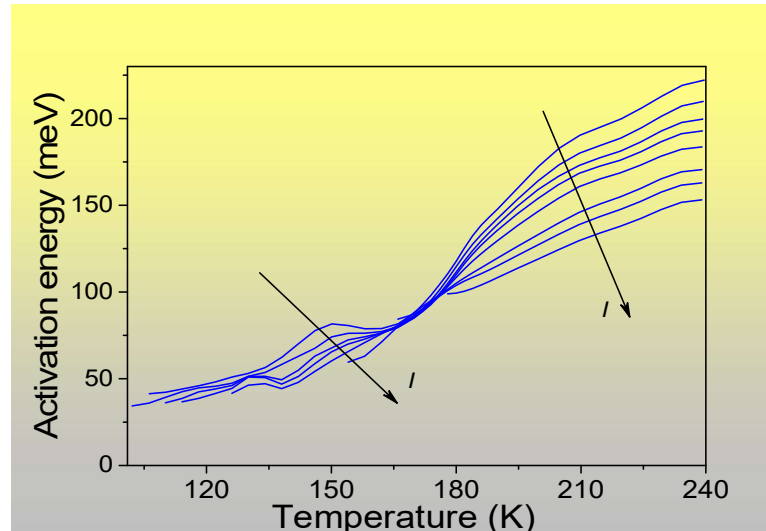
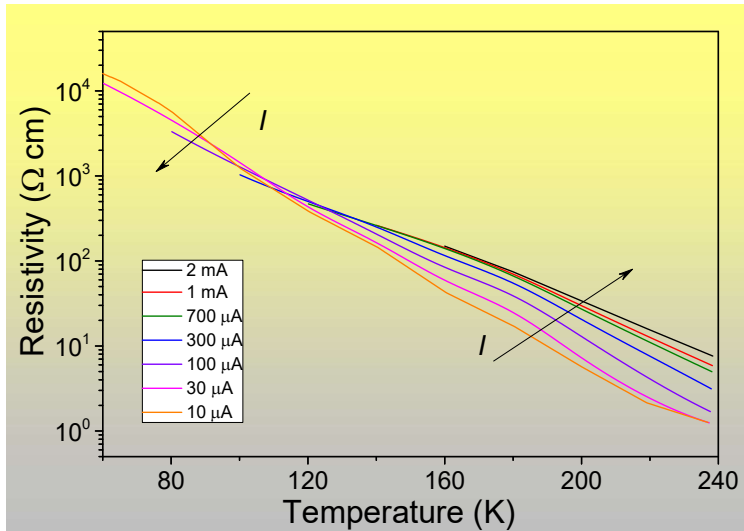
$$\Delta S \approx k_B \ln \frac{N}{N-n} + n \ln \frac{N-n}{n}$$

$$\approx k_B \ln \frac{n^N}{N!} \approx k_B n \ln \frac{N}{n} \approx k_B n \ln N$$

$$\Delta S = k_B \frac{\Delta H}{\hbar\omega_0} \ln N \quad \text{Meyer-Neldel rule}$$

$$T_{MN} = \frac{\hbar\omega_0}{k_B} \ln N \quad N - \text{coupling constant}$$

Meyer-Neldel rule



$$\rho(T) = \rho_0 \exp\left(\frac{E_a}{k_B T_{MN}}\right) \exp\left(-\frac{E_a}{k_B T}\right)$$

$$\rho_0(T) = \rho_0 \exp\left(\frac{E_a}{k_B T_{MN}}\right)$$

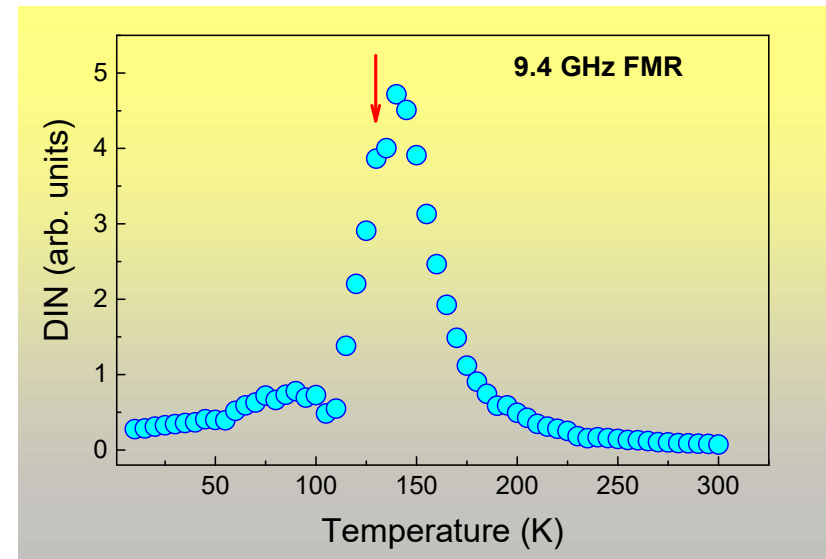
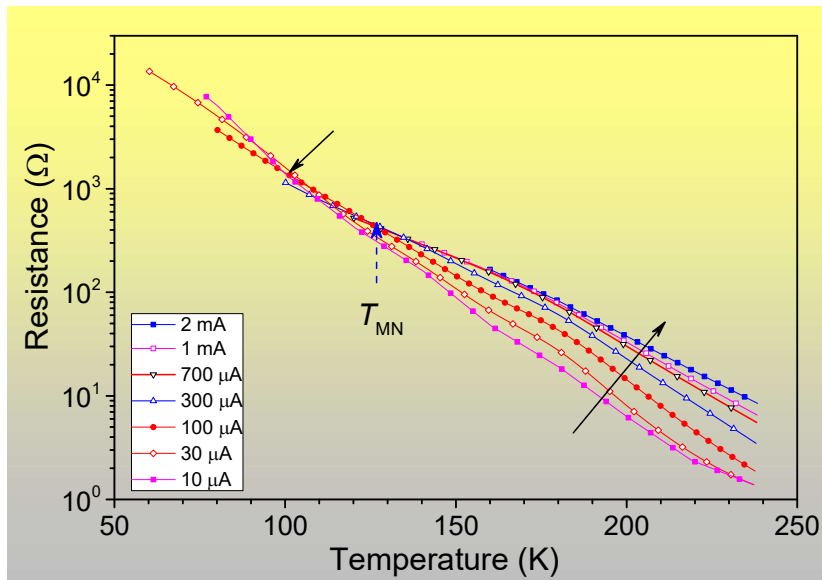
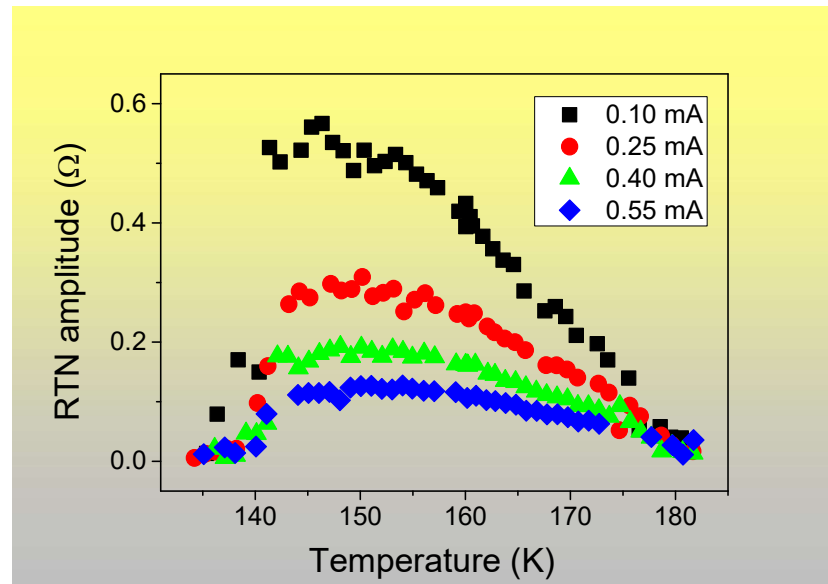
$$\ln \rho_0 \sim E_a$$

Macroscopic Random Telegraph Noise Conclusions

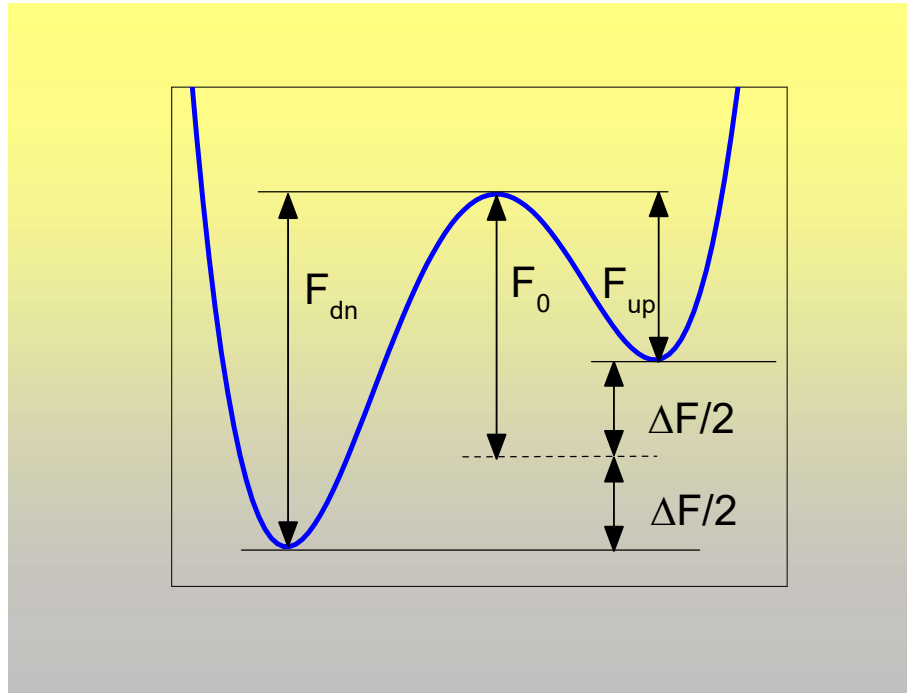
- Macroscopic RTN in superconductors appears due to dynamic coexistence of ordered and disordered phases of vortex matter. Disordered vortex matter is injected into a sample through the edges, due to vortex edge contamination mechanism.
- Macroscopic RTN in CMR manganites is typically associated with strong PS and coexistence of phases with markedly different magnetic and electronic properties or, alternatively, with fluctuations of magnetic moments in large FM domains around T_c . Novell, robust M-RTN is due to dynamic current redistribution assisted by Meyer-Neldel feedback mechanism.
- The common denominator to M-RTN in strongly correlated systems is phase separation resulting in dynamic coexistence of phases with different properties.

Can Macroscopic Random Telegraph Noise appear in physical systems which are not strongly correlated?

M-RTN amplitude



Free energy difference



$$\tau_{up} = \tau_{0_{up}} e^{\frac{F_0 + F/2}{k_B T}}$$

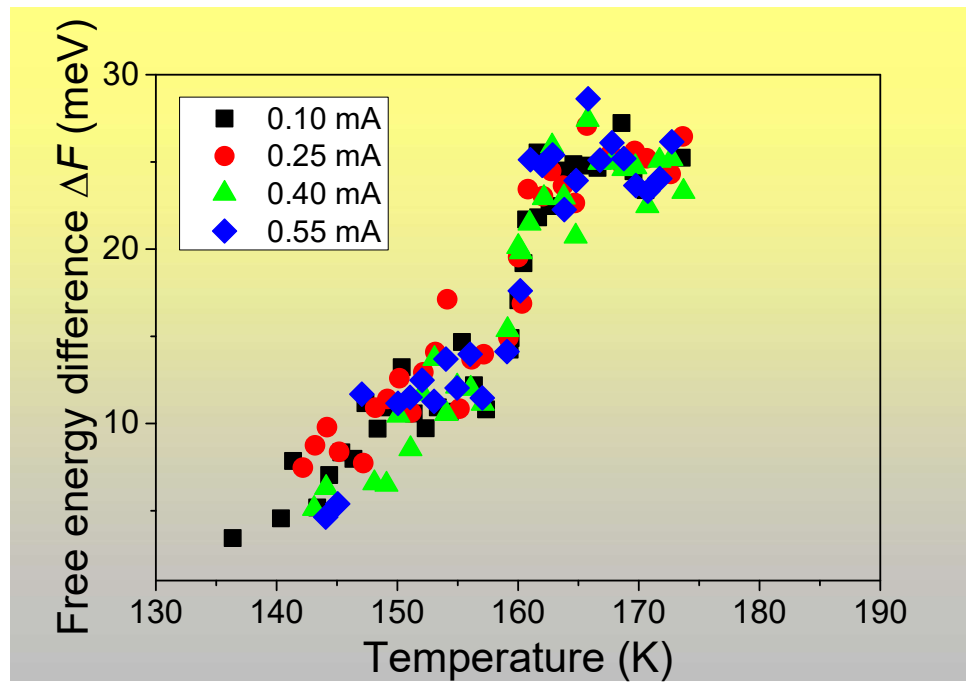
$$\tau_{dn} = \tau_{0_{dn}} e^{\frac{F_0 - F/2}{k_B T}}$$

$$r = \tau_{up}/\tau_{dn}$$

$$\tau_{0_{up}} = \tau_{0_{dn}}$$

$$\Delta F = k_B T \ln r$$

TLF Thermodynamics

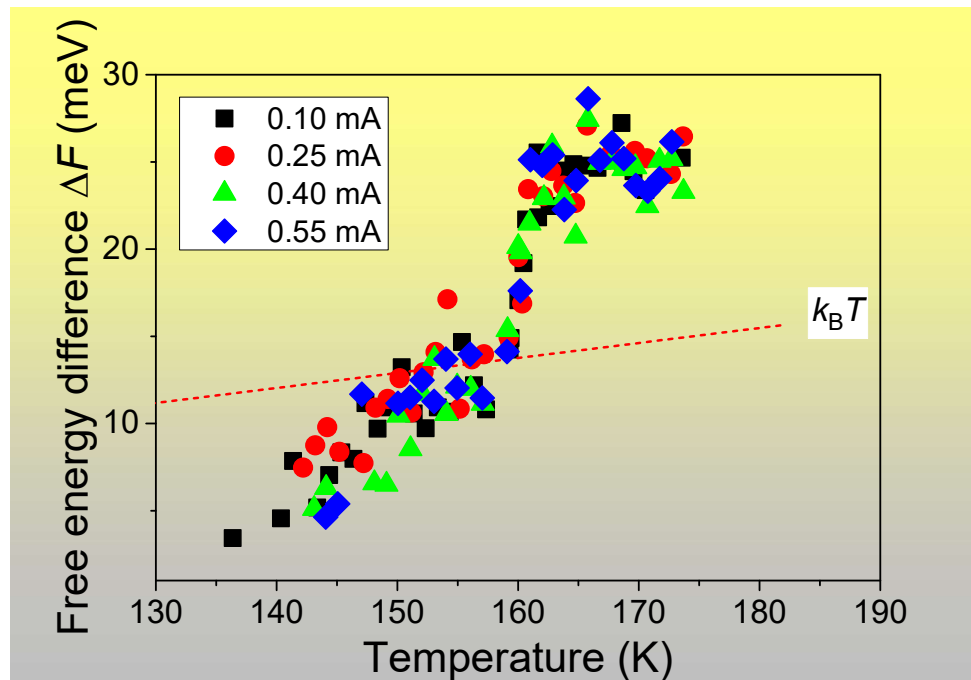


$$\Delta F = E - T\Delta S$$

$$\Delta S = -\frac{1}{k_B} \frac{\partial \Delta F}{\partial T}$$

$$\Delta S = 7.8 \pm 0.5$$

TLF Thermodynamics

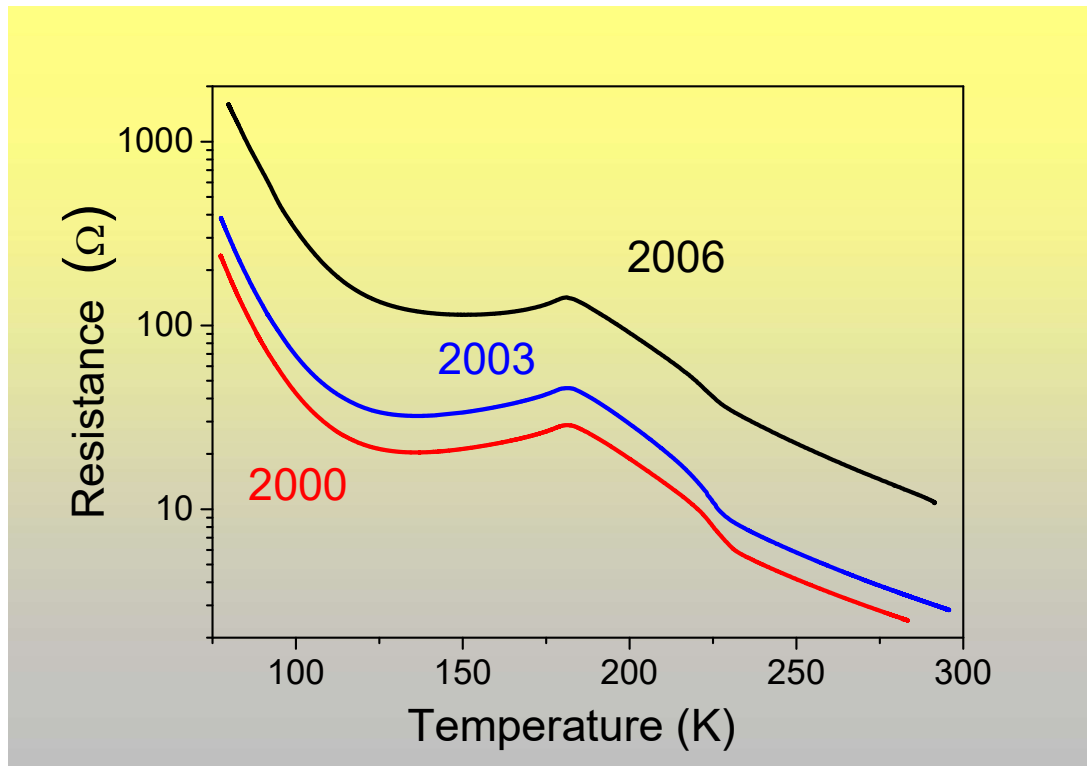


$$\Delta F = E - T\Delta S$$

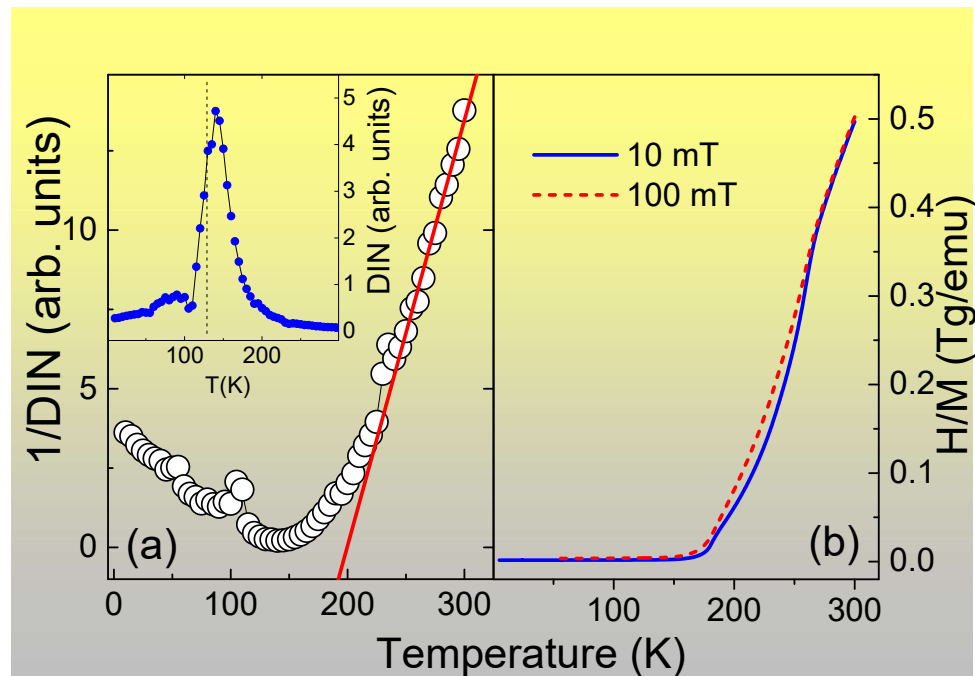
$$\Delta S = -\frac{1}{k_B} \frac{\partial \Delta F}{\partial T}$$

$$\Delta S = 7.8 \pm 0.5$$

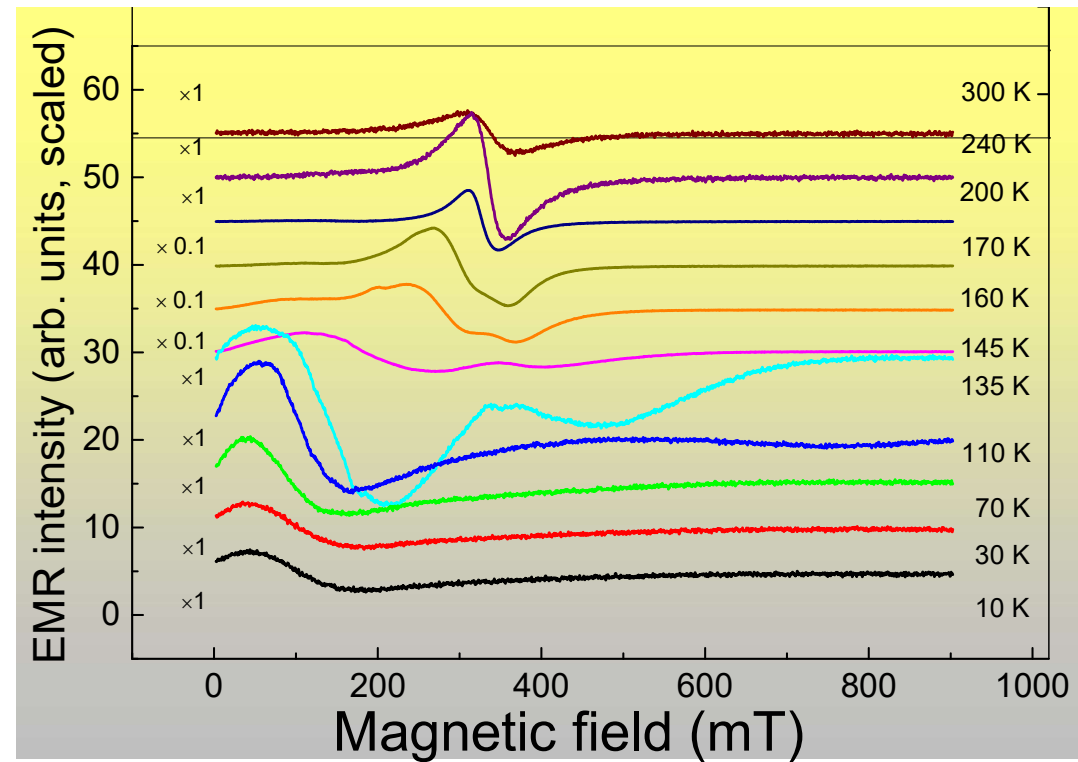
LCMO 0.18 - Ageing



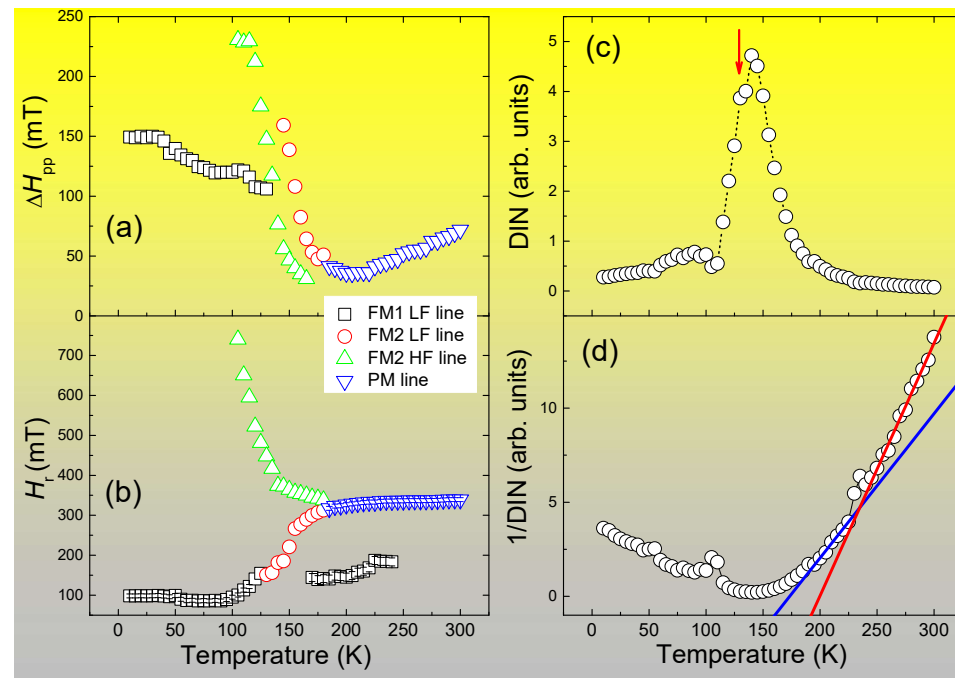
Susceptibility



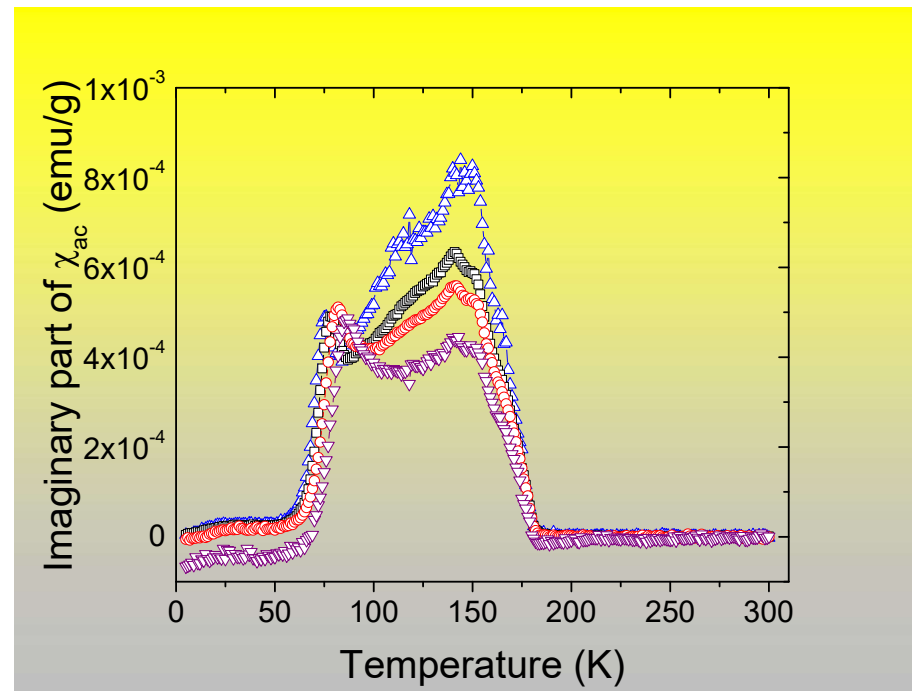
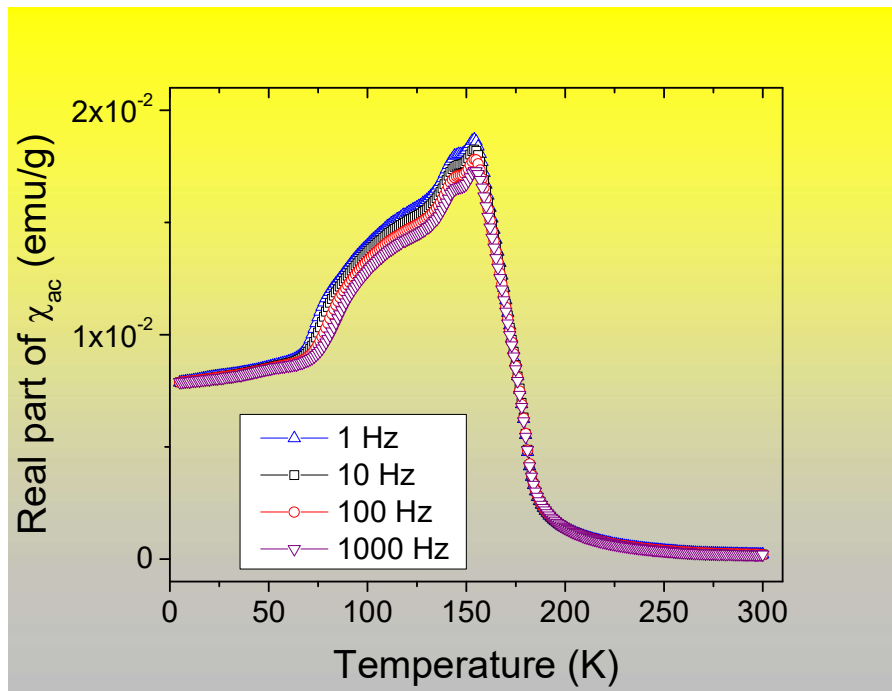
EMR spectra



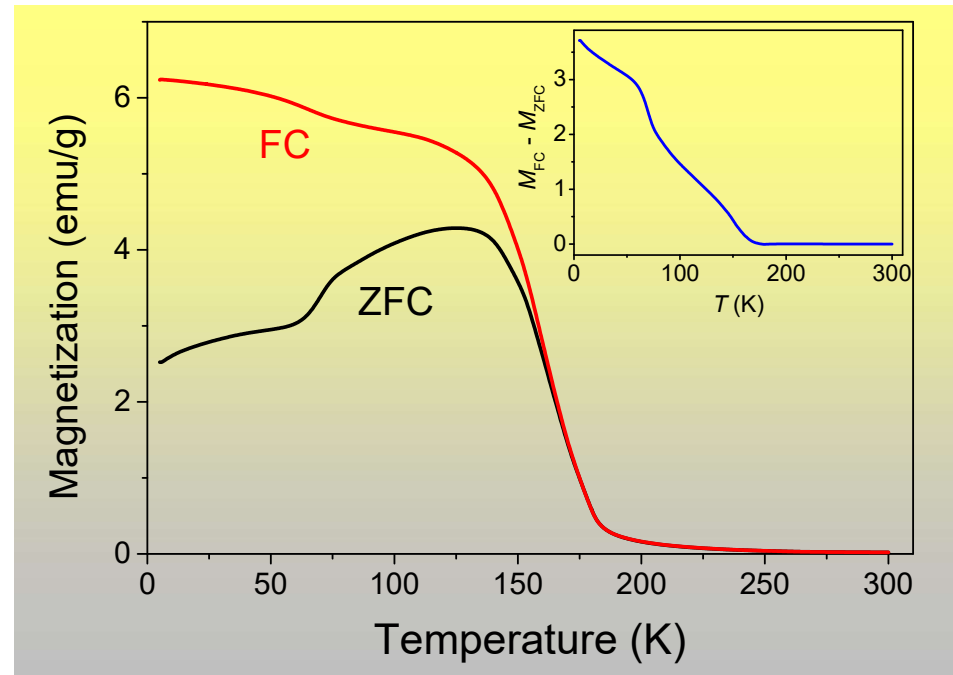
EMR parameters



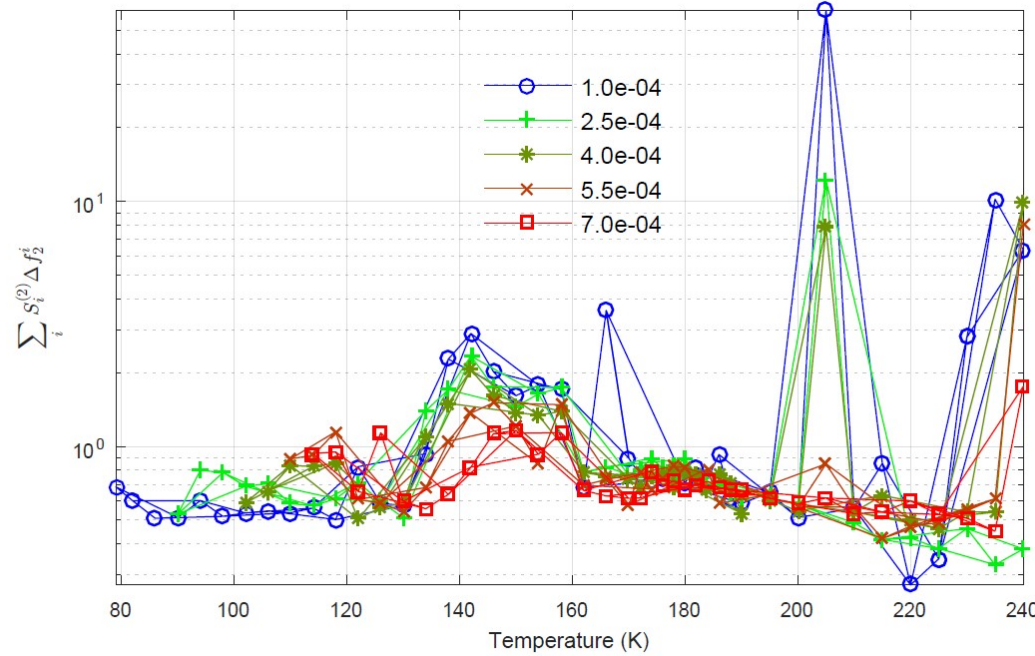
LCMO 0.14 AC susceptibility



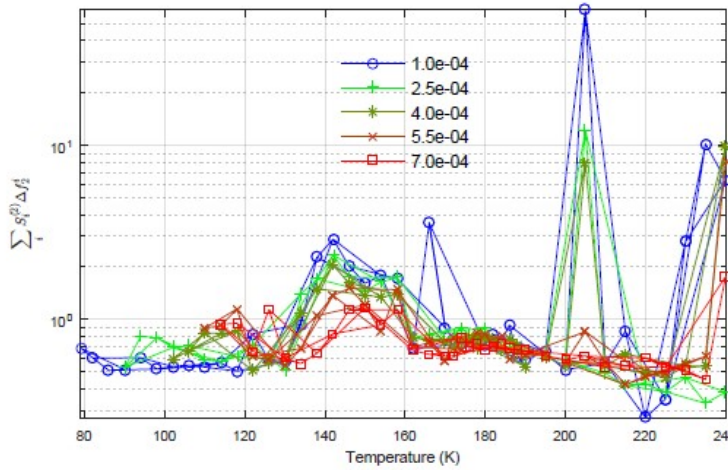
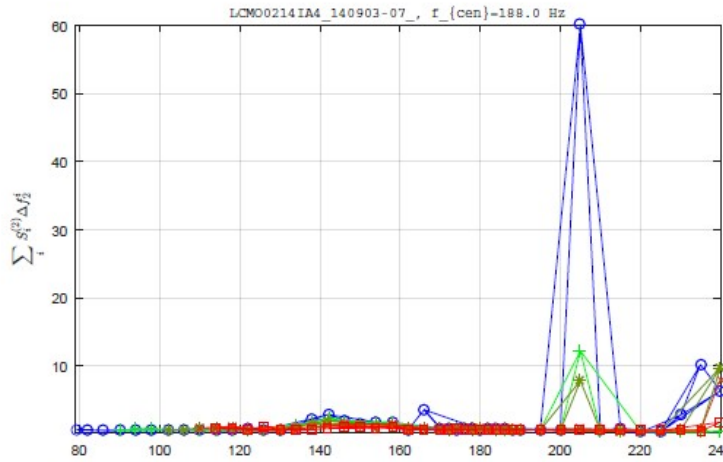
LCMO 0.14 magnetization



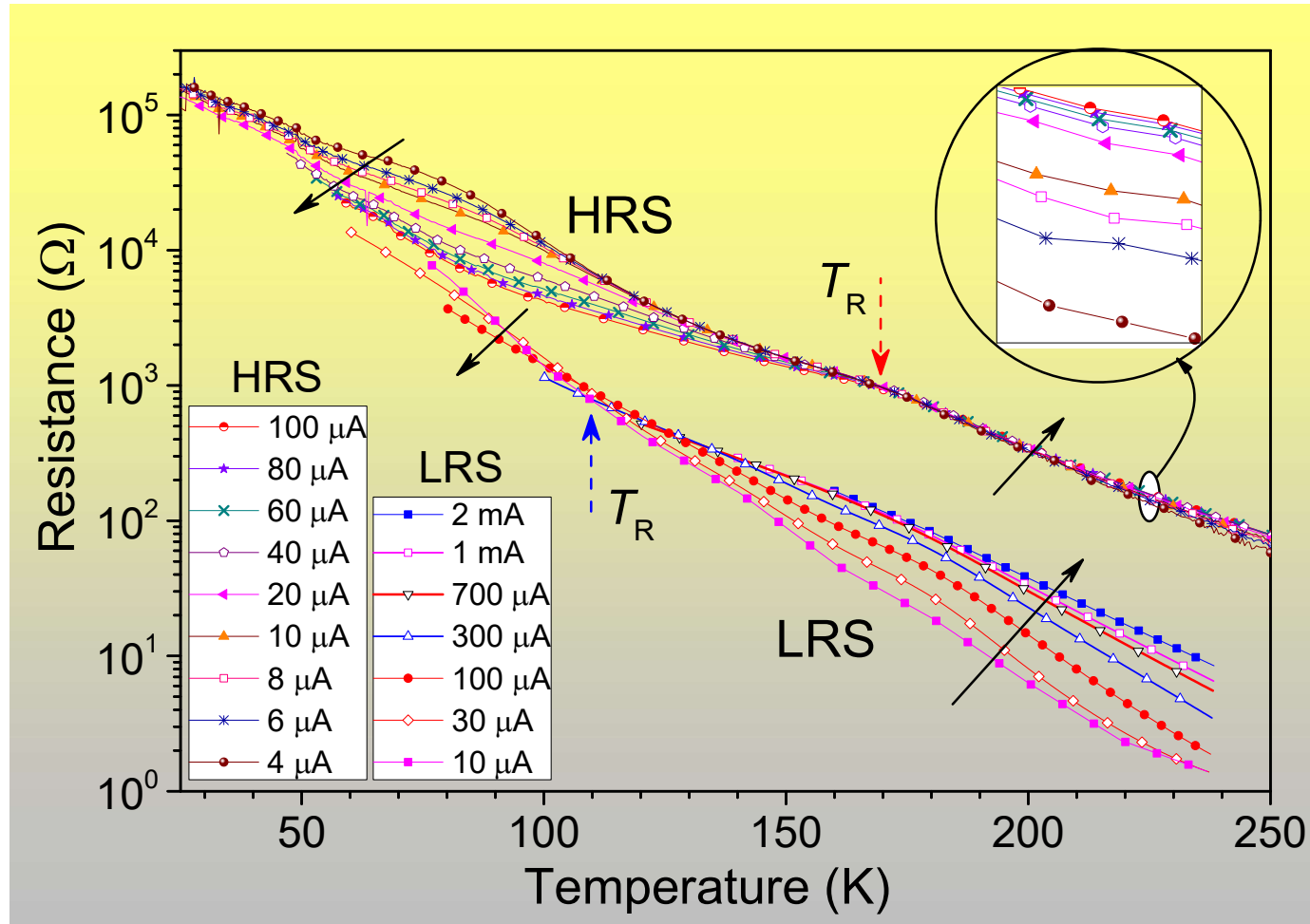
Integrated second spectrum



Integrated second spectrum

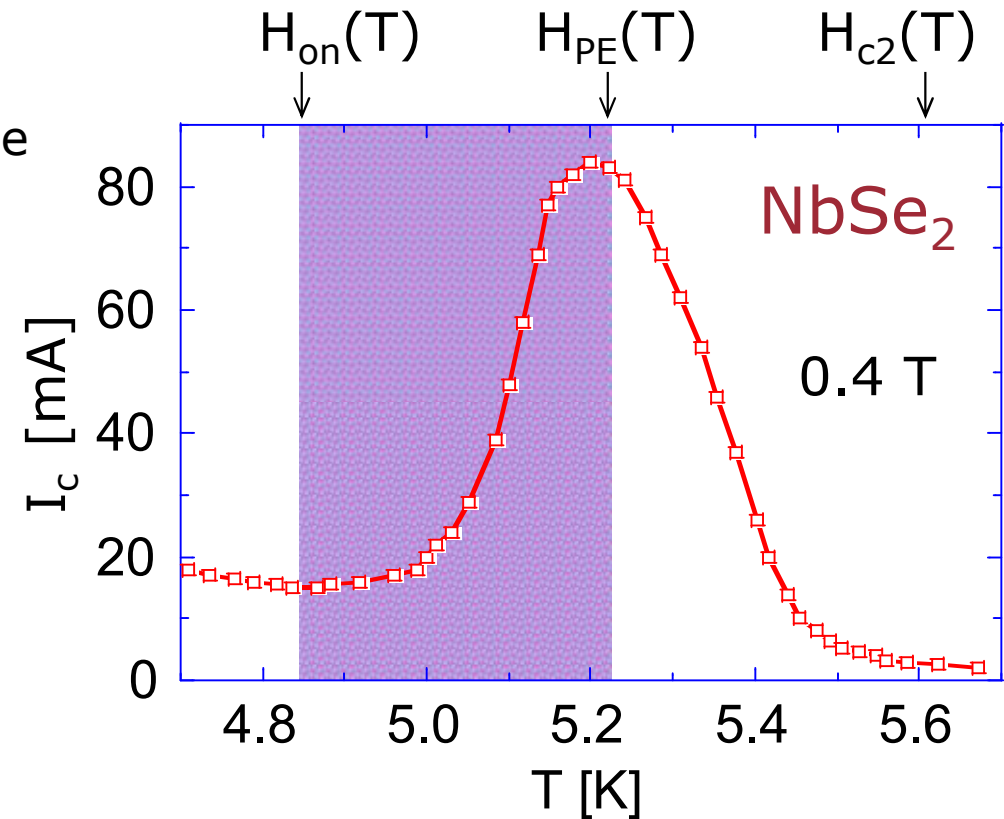


$R(T,I)$ $\text{La}_{0.86}\text{Ca}_{0.14}\text{MnO}_3$ single crystal



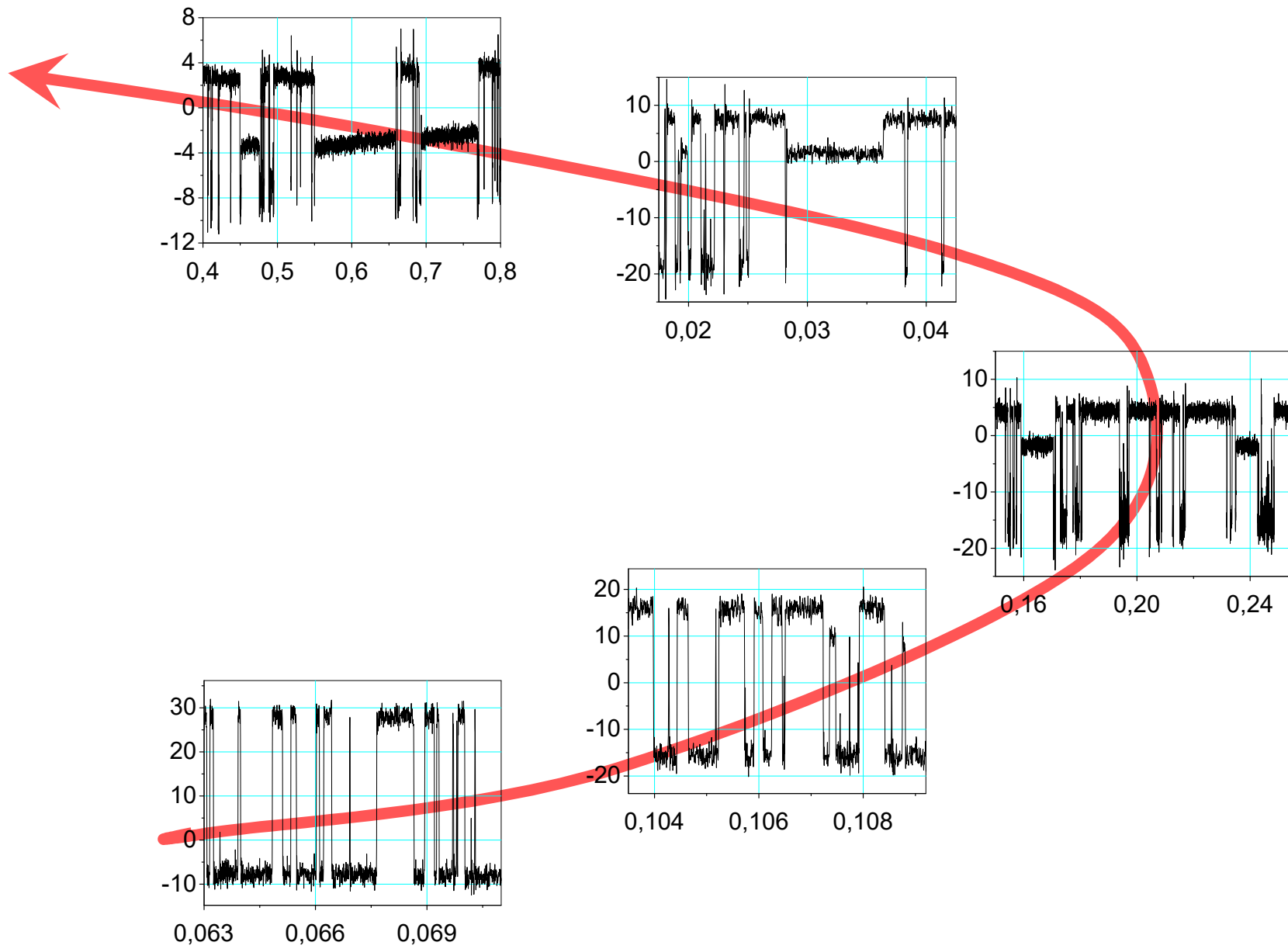
Anomalous vortex phenomena in the vicinity of peak effect.

- History-dependent dynamic response
- Memory effects
- Frequency dependence
- Suppression of *ac* response by small *dc* bias
- Negative differential resistance
- Slow voltage oscillations
- Low-frequency noise

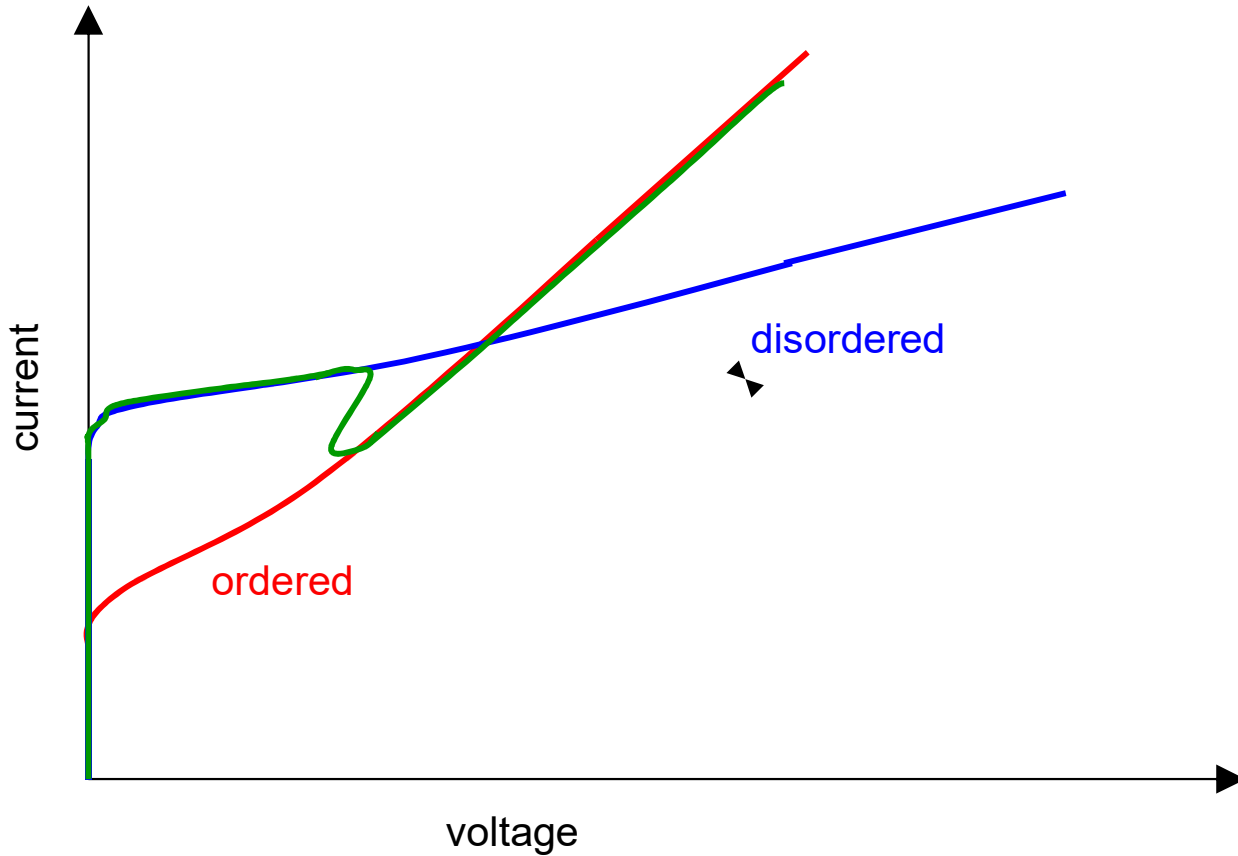


Ph.D. thesis Yossi Paltiel – Edge contamination model

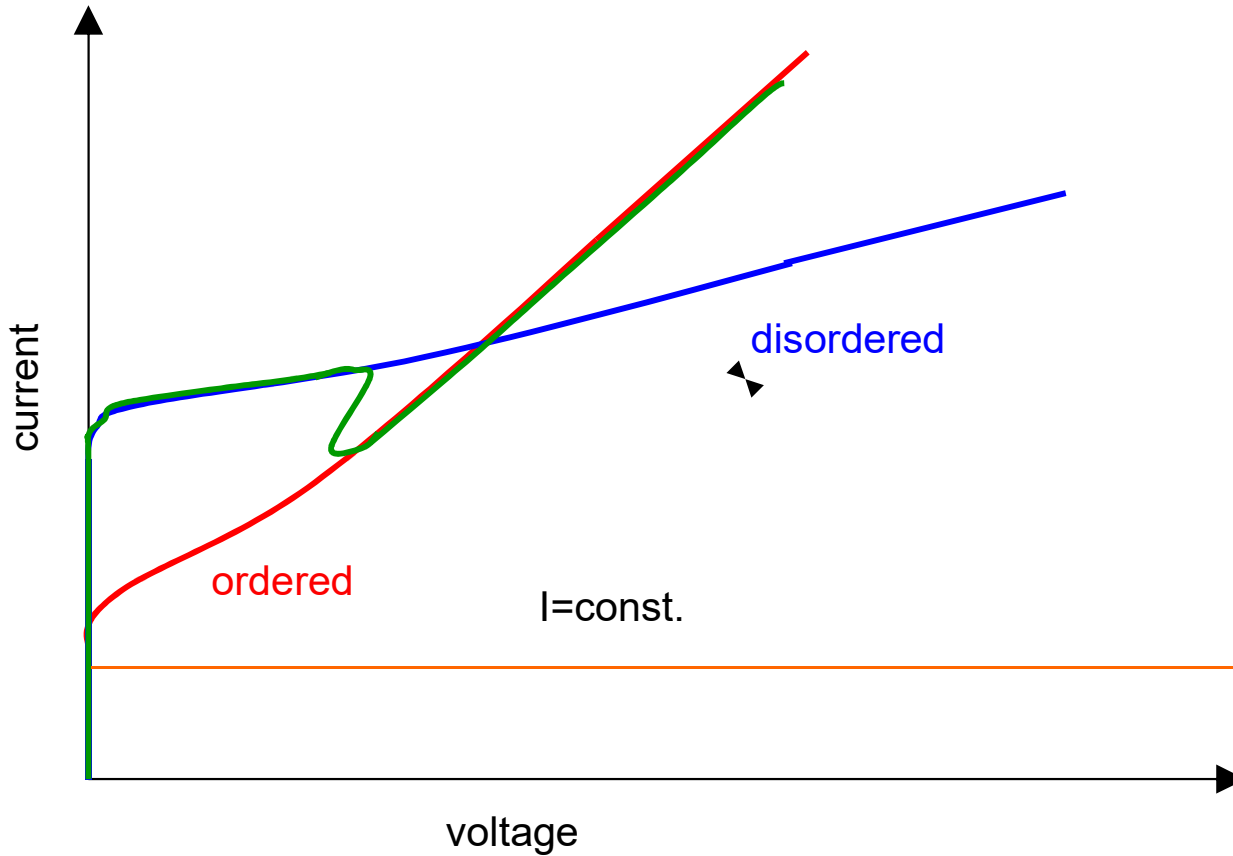
Amplitude modulated M-RTN



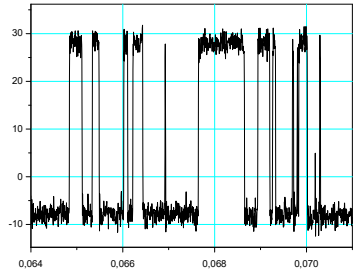
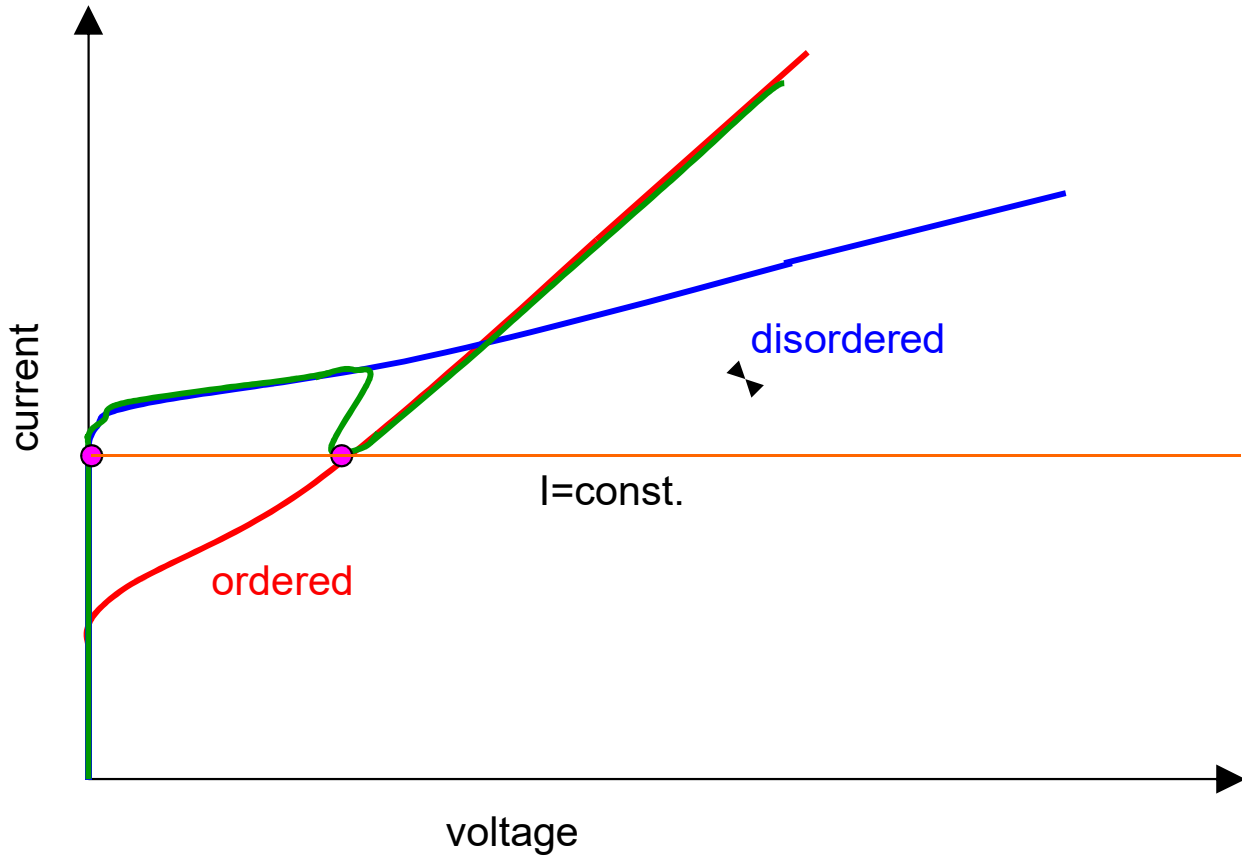
Amplitude modulated M-RTN



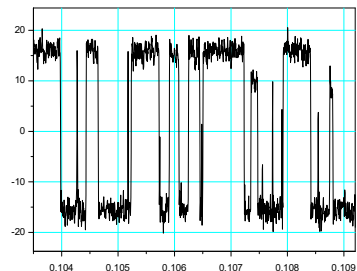
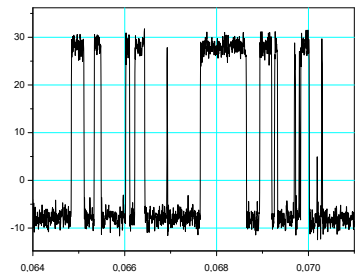
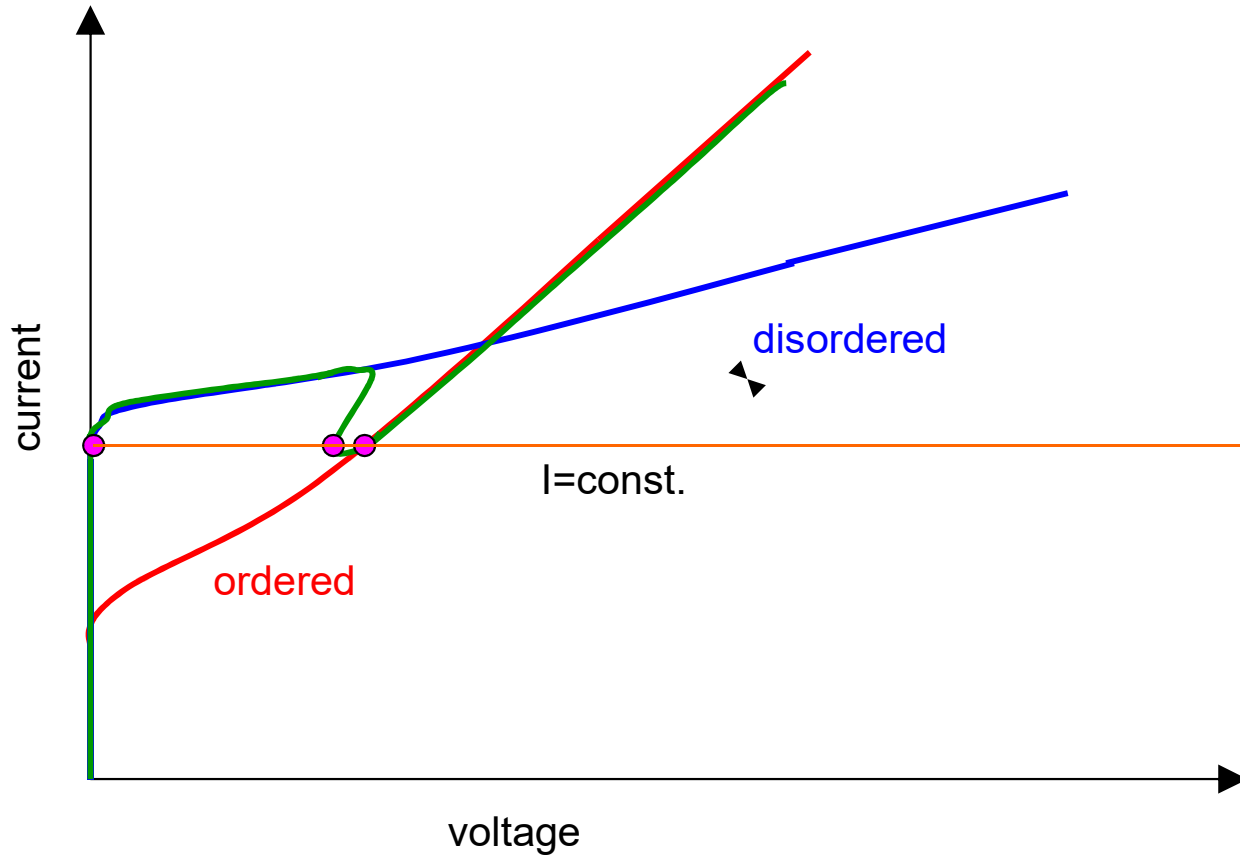
Amplitude modulated M-RTN



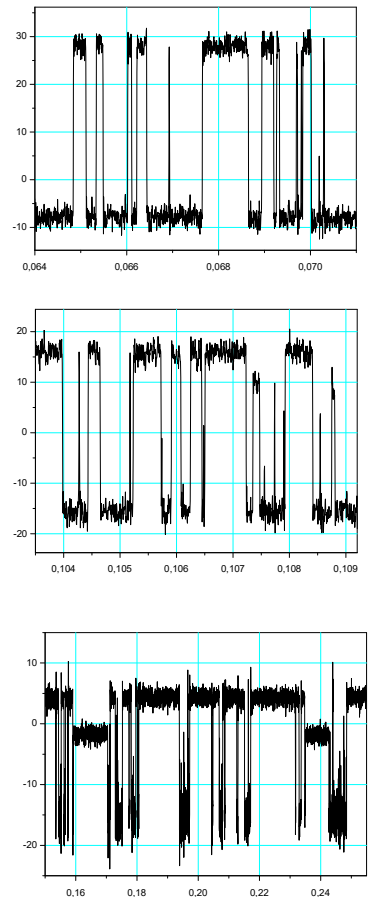
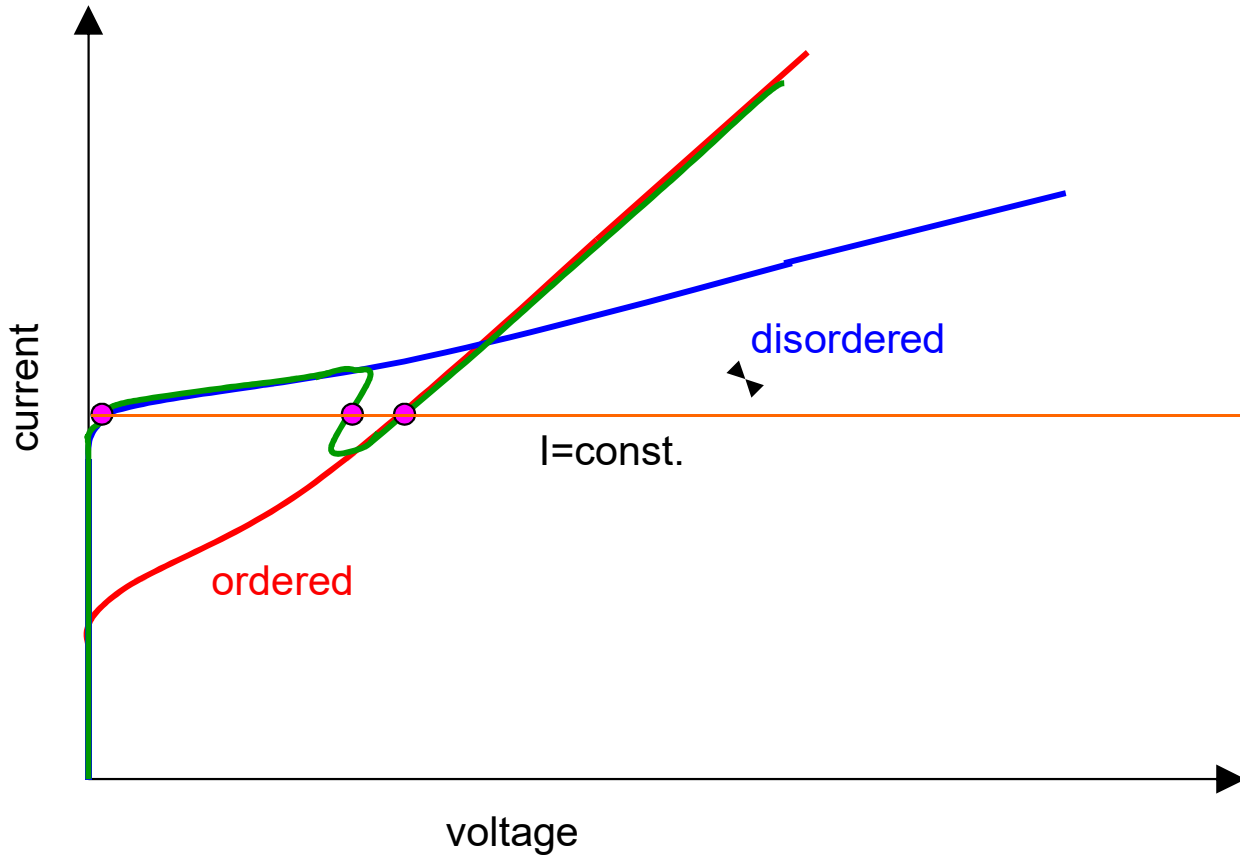
Amplitude modulated M-RTN



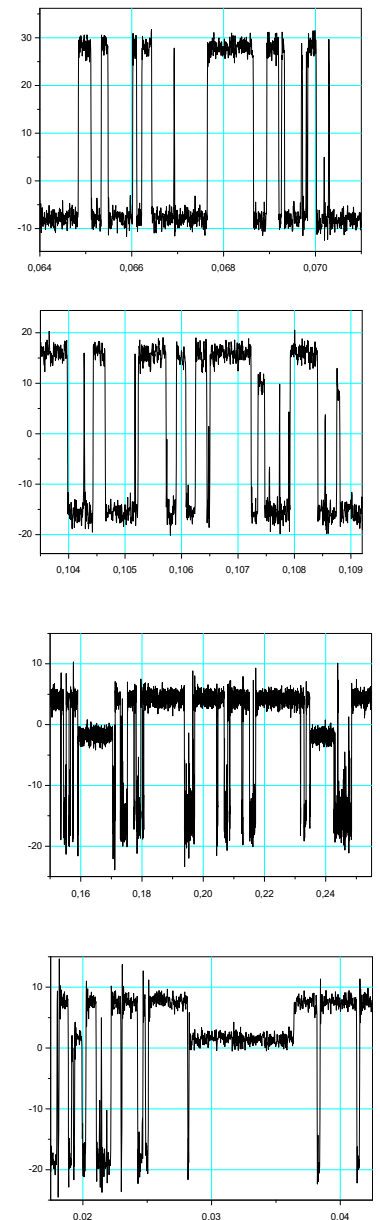
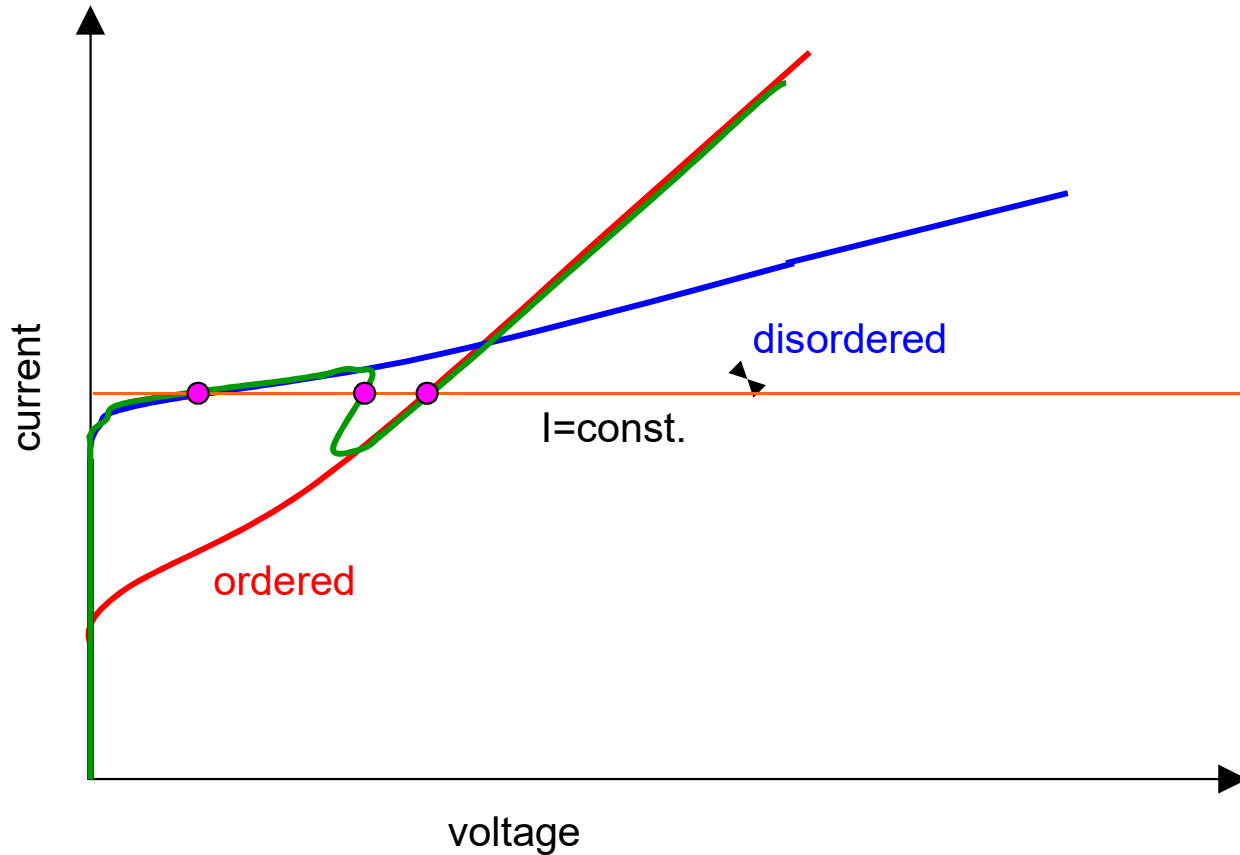
Amplitude modulated M-RTN



Amplitude modulated M-RTN



Amplitude modulated M-RTN



Amplitude modulated M-RTN

